Title

Discrete Systems in Quantum and Statistical Mechanics

Author

Shea, Meredith

Publication Date

2022

Peer reviewed|Thesis/dissertation

Discrete Systems in Quantum and Statistical Mechanics

by

Meredith Shea

A dissertation submitted in partial satisfaction of the

requirements for the degree of

Doctor of Philosophy

in

Mathematics

in the

Graduate Division

of the

University of California, Berkeley

Committee in charge:

Professor Nicolai Reshetikhin, Chair
Professor Ian Agol
Professor Robert Littlejohn

Spring 2022

Discrete Systems in Quantum and Statistical Mechanics

Abstract

Discrete Systems in Quantum and Statistical Mechanics

by

Meredith Shea

Doctor of Philosophy in Mathematics

University of California, Berkeley

Professor Nicolai Reshetikhin, Chair

Here we consider operators in the physics literature and explore their discretized counterparts for a better understanding of their behavior. In chapter 2, we discretize a standard Hamiltonian model from quantum mechanics and, in this setting, develop a discretized Gelfand-Yaglom formula. From this discrete set up we are able to develop an alternative regularization for the determinant of a class of operators. We refer to this as the lattice-regularization.

In chapters 3 and 4 we develop connections between the asymptotics of the inverse of two different operators: the Kasteleyn operator with interface and the Dirac operator with interface. The definition of these operators are given in their respective chapters. While the former is operator acting on a discrete space and the latter is acting on the plane, there are well established connections between the two [14]. Moreover, in chapter 3, we give a complete picture of the asymptotics across the interface when one half of the lattice is weighted critically and the other half is weighted non-critically.

Acknowledgments

First and foremost I would like to thank my advisor, Kolya Reshetikhin, for his unwavering guidance and for periodic reminders that I am only human. I would like to thank Leon Takhtajan, Sylvie Corteel, Zhongyang Li, and Matthew Nicoletti for valuable conversations that contibuted greatly to the work seen here. I also am grateful for the hospitality I was afforded at the ETH Institute of Theoretical Physics and at the Centre de Recherches Mathématiques. Also, thank you to my other committee members, Ian Agol and Robert Littlejohn, for taking the time evaluate this work. This work was partially supported by NSF grants DMS-1664387, DMS-1902226 and DMS-2000093.

I am especially grateful for the love and support of my parents, Jean and Jim, and my fiancé, Kayla, throughout this long journey. Thank you for pretending that my ramblings made any sense to you. Thank you to Rachel and Ferin, for always escaping with me in the woods; Nic, for being my forever office mate; and Asha, for being by my side these past two years. Also thank you to my best friends (you know who you are) for being my rocks – I'm sorry there is no 'Dith theorem' to show for it.

Contents

List of Figures

Chapter 1

Introduction

The broad goal of this exposition is to investigate the properties of operators that arise in important systems in quantum and statistical mechanics. In particular, we use the relationships between continuous systems and their discrete counterparts as a tool of investigation. We start in chapter 2 by using a discretized system to formulate an alternative regularization for a class of continuous differential operators. Then, in chapters 3 and 4, we compare the asymptotic behavior of a particular Kasteleyn operator and a Dirac-like operator, where the former is on operator acting on a discrete domain (vertices of a lattice) and the latter is a operator that acts on spinors in $\mathbb{R}^2$. Below we summarize the main results of this paper.

We begin in chapter 2, where we study a new regularization for the determinants of a class of differential operators through the lens of quantum mechanics and a Gelfand-Yaglom formula. Gelfand and Yaglom first inspired this type of formula by relating the evaluation of a certain class of exponential integrals to a Sturm-Loiusville problem in [9]. The original formula has since been refined to relate the regularized determinant of an elliptic operator to the solution of an initial value problem. A presentation of this formula that emphasizes its connection to quantum physics can be seen in [23]. Moreover, this modern take on the Gelfand-Yaglom formula is fully describe in section 2.3.

We begin by developing a discretized quantum system in section 2.6 and the corresponding discretized action. From this set up we are able to derive a discretized generalized Gelfand-Yaglom formula. This formula is detailed in Theorem 2.5. We then used the continuum limit of this discretized set up to define an alternative regularization of the determinant of the original continuous operator. We call this alternative regularization the lattice-regularization, which is defined in Definition 2.1.

In this discretized Hamiltonian set up, the lattice regularization is often convergent and presents a potentially easier way to compute the regularized determinant of the Hamilton-Jacobi operator. Note the distinction between Hamiltonian and Lagrangian formalism is important here. This can be immediately seen in section 2.6.2, as the determinant of the discrete Laplacian does not converge naively in the continuum limit. This may motivate the Hamiltonian formalism as the more natural setting to consider these operators.

In many classical examples, we can show that the lattice regularization is equivalent, up to a multiplicative constant, to the zeta-regularization. This is accomplished in Corollary 2.6.1. Moreover, the lattice-regularization can be applied to examples that are not contained within the scope of the usual Gelfand-Yaglom formula, although convergence of the lattice-regularization may no longer be obvious.

In chapter 3, we turn our focus to a problem regarding dimer models. A *dimer configuration*, or perfect matching, of a graph is a subset of the edges which covers every vertex exactly once. Given a graph, one assigns a positive weight to each edge. The probability of a random dimer configuration is proportional to the product of all the edge weights of the edges included in the configuration. A *dimer model* studies the random dimer configurations of a graph.

For case of uniform edge weights, in other words each dimer is equally likely, solutions to the dimer model on regions of the square and hexagonal lattice are well understood. Moreover, in the case of periodic weightings, the dimer model has been studied for many cases of the square lattice [13, 6, 5]. There are also similar results regarding isoradial graphs [14, 19], and the more general Rail Yard graphs [2]. In general, less is known about dimer models when the weightings are not periodic. In some instances, non-periodic weightings can still be expressed as a *Schur process* and exact solutions are known. Some examples of this can be seen in [21, 1, 3, 2].

Of principle interest in the study of dimer models is understanding the asymptotic behavior of the model. Specifically, when we allow the model to become large and re-scale appropriately, the *height function* (a function associated to the faces of the graph for a given dimer configuration) tends to a deterministic limit shape which describes the global behavior of the model [15, 16]. The limit shape of a model illustrates the different phases that occur. In particular, the phases possible are deterministic (frozen), critical (liquid or rough), and non-critical (gas or smooth). Depending on the weights in a given dimer model, the model can exhibit a single phase or a mix of some or multiple phases.

A classic example of the limit shape of a dimer model is the arctic curve phenomenon of the uniform Aztec diamond [7, 10]. For this model, an elliptic curve separates a deterministic (the outside) and critical region (the interior). In the critical region, the height fluctuations are known to converge to a *Gaussian free field* [12, 22]. More complicated limit shapes of the Aztec diamond have been studied in [6, 5].

In chapter 3, we consider the dimer model on the infinite square lattice with, what I refer to as, an interface weighting. This weighting is non-periodic in the horizontal direction. The interface weighting is motivated by combining a lattice weighting which exhibits critical behavior (on an infinite planar lattice) with a lattice weighting that exhibits non-critical behavior (on an infinite planar lattice). These two regions are separated by an interface. This weighting is formally defined in section 3.3.1.

The main result of this chapter is as integral form of the inverse Kasteleyn operator for this dimer model, which is presented in Theorem 3.1. The rest of the chapter is dedicated to studying the asymptotic behavior of this inverse operator in order to gain an understanding of the limit shape of the particular dimer model. Of note, the lattice behaves incredibly predictably in the asymptotic limits. On the 'critical' side of the lattice, the decay is inverse in distance, while on the 'non-critical' side of the lattice the decay is exponential in distance.

Lastly, in chapter 4 we turn our attention to, what we refer to as, the Dirac operator with interface. This operator was motivated by the operator studied in chapter 3 as well as the connections between the Dirac operator and Kasteleyn operator discussed in [14].

The Dirac operator with interface is defined generally in section 4.1. Moreover, an integral form of the Green's function for this operator is given in Theorem 4.1. In the rest of the chapter, we focus on the Dirac operator with interface where the interface separates a massive and massless Dirac operator. This operator in particular is motivated by the case in chapter 3 of the Kasteleyn operator with non-critical/critical interface. In section 4.3, we study the asymptotics of the Green's function for the Dirac operator with massive/massless interface.

While the Kasteleyn operator does not naively converge to the Dirac operator with interface, the asymptotics of these two operators are resoundingly similar. These connections are discussed in section 4.4 in moderate detail.

Chapter 2

Regularized Determinants

Here we give an alternative regularization for the determinant of a class of differential operators. We first discuss necessary preliminary information in sections 2.1-2.4, including a useful formulation of the Gelfand-Yaglom formula. Then we define a discretize quantum mechanics system in section 2.5 and prove a discretized generalize Gelfand-Yaglom formula in Theorem 2.1. In sections 2.6 and 2.7, we prove the operator that is discretized in section 2.5 converges to its continuous counterpart. By way of this convergence, we are able to define the lattice-regularized determinant.

2.1 Quantum mechanics formalism

To understand the motivation of the problem presented in this chapter, it will be useful to understand some quantum mechanics. In this section, we introduce two common set ups used in quantum mechanics from the perspective of a mathematician. In both set ups described below, we will consider the classical problem from physics:

Consider a one-dimensional system with a particle of mass m and a potential energy V (that only depends on position), what are the equations of motion and statistics of the system?

Lagrangian formalism

We will define the path of the particle by the function $q(t) : [0, T] \to \mathbb{R}$, where $q(t)$ describes the position in one-dimensional space of the particle at time t. We will also use the standard notation $\dot{q}(t) = dq(t)/dt$. With this in mind we first define the *Lagrangian* of the system at hand,

$$L\left(q(t), \dot{q}(t), t\right) = \frac{m}{2}\dot{q}(t) - V\left(q(t)\right) \tag{2.1}$$

From the Lagrangian we are able to define the action functional of the system,

$$S\left[q(t)\right] = \int_0^T \left(\frac{m}{2}\dot{q}(t)^2 - V\left(q(t)\right)\right) dt \tag{2.2}$$

The action functional is a map from the space of all possible paths to the underlying field. For the sake of this work, it is not necessary to be specific on what the space of possible paths entails.

We will call the path that minimizes the action functional the critical point of the action and denote it $q_c(t)$. In particular, the critical point is the solution of the ODE,

$$m\ddot{q}(t) = -V'\left(q(t)\right) \tag{2.3}$$

One way to understand that this is the critical point is by computing the variation of the action functional,

$$\delta S\left[q(t)\right] = \int_0^T \left(\frac{\partial L}{\partial q(t)} - \frac{d}{dt}\frac{\partial L}{\partial \dot{q}(t)}\right)\delta q\, dt \tag{2.4}$$

Note that the above is a functional derivative and thus is an abuse of notation. At the critical point $\delta S[q_c(t)] = 0$ and so, since δq is not zero, it hold that

$$\frac{\partial L}{\partial q_c(t)} - \frac{d}{dt}\frac{\partial L}{\partial \dot{q}_c(t)} = 0 \tag{2.5}$$

And the above is equivalent to (2.3). We call equation (2.5) the *Euler-Lagrange equation.*

Hamiltonian formalism

Instead of considering the space of paths, in Hamiltonian formalism we consider the phase space of a system. In the phase space, we express a path in terms of its coordinates on the cotangent bundle of $\mathbb{R}$. We let $\tilde{\mathbf{q}}(t) = (q(t), p(t)) : [0, T] \to \mathbb{R}^2$ and write the Hamilton-Jacobi action as,

$$\tilde{S}\left[\tilde{\mathbf{q}}(t)\right] = \int_0^T \Big(p(t)\dot{q}(t) - H\left(p(t), q(t)\right)\Big)dt \tag{2.6}$$

We call $H\left(p(t), q(t)\right)$ the *Hamiltonian* of the system, which is simply the Legendre transform of the Lagrangian. For the system expressed by the Lagrangian in equation (2.1) the equivalent Hamiltonian is,

$$H\left(p(t), q(t)\right) = \frac{p(t)^2}{2m} + V\left(q(t)\right) \tag{2.7}$$

As in the Lagrangian formalism, we may compute the equations of motion of the critical point by minimizing the variation of the action functional. In doing so we recover Hamilton's equations for the system at hand,

$$\dot{q}_c(t) = \frac{1}{m}p_c(t) \tag{2.8}$$
$$\dot{p}_c(t) = -V'\big(q_c(t)\big) \tag{2.9}$$

An immediate difference we observe in the Hamiltonian formalism is that the equations of motion are a system of first order equations, while in the Lagrangian formalism the equations of motion are a single second order equation.

2.2 Zeta-regularized determinants

We now wish to discuss a certain type of regularized (or functional) determinant that will be necessary to understand Gelfand-Yaglom formulas. Regularized determinants are a generalization of determinants of matrices. Where matrices are operators acting on finite dimensional spaces, we can think of differential operators as acting on some infinite dimensional space. Understanding determinant in this setting is still insightful, however we have to amend definitions in order to count for conditions of convergence.

Here we would like to define the ζ-regularized determinant of a class of operator. Let L be a differential operator with a discrete spectrum that is bounded from below. We start by remove any zero eigenvalues and enumerate the spectrum, $\lambda_1 \leq \lambda_2 \leq \cdots \leq \lambda_n \leq \cdots$. Assuming the following series converges for sufficiently large $\Re(s)$, we define the ζ-function of the operator L to be,

$$\zeta_L(s) = \sum_i \frac{1}{\lambda_i^s}$$

Then the ζ-regularized determinant is defined as,

$$\det{}_\zeta(L) = e^{-\zeta_L'(0)}$$

where we must analytically continue the derivative of the ζ-function of the operator to the point $s = 0$. Note that this is possible by Seeley's theorem, which states that the zeta-function of an elliptic operator extends to a meromorphic function in the complex plane and the origin is always a regular point. In the case of second order differential operators, see [23] and [17] for examples of computing ζ-regularized determinants.

2.3 The Gelfand-Yaglom formula

The evaluation of certain integrals with respect to the Wiener measure is first studied in [9]. It was found that the solution to certain integrals of exponentials can be expressed in terms of a solution to a Sturm-Liousville problem. Later this formula was interpreted as a relation between the regularized-determinant of an elliptic operator and the solution to an initial value problem. In particular, this formula can be understood in the context of quantum mechanics.

In this section, we will consider the system described by the Lagrangian in (2.1) and Hamiltonian in (2.7). The goal of this section is to motivate and state the Gelfand-Yaglom formula in both the Lagrangian and Hamiltonian formalism.

The statement in Lagrangian formalism

Let us start by considering the action stated in equation (2.2). Taking the second variation of the action functional at the critical point, we obtain the expression

$$\delta^2 S\left[q_c(t)\right] = \int_0^T \delta q \, A \, \delta q \; dt \tag{2.10}$$

where A is the differential operator,

$$A = -\frac{d^2}{dt^2} - \frac{1}{m} V''\left(q_c(t)\right) \tag{2.11}$$

that is equipped with Dirichlet boundary conditions. Recall the critical point is the path $t \mapsto q_c(t)$ that satisfies the equation give in (2.3). In particular, we will consider the critical point to have the following initial conditions,

$$q_c(0) = q \qquad \dot{q}_c(0) = \frac{p}{m}$$

The Gelfand-Yaglom formula states,

$$\frac{\partial q_c(T)}{\partial p} = \frac{1}{2m} \det{}_\zeta(A) \tag{2.12}$$

where p is the parameter defined above. A proof of this statement can be found in [23], among other places.

The statement in the Hamiltonian formalism

We would like to formulate a similar statement to the one in (2.12) that is expressed in Hamiltonian formalism instead. Let us use $\tilde{\mathbf{q}}_{\mathbf{c}}(t) = (q_c(t), p_c(t))$ to denote the solution to Hamilton's equations, equations (2.8) and (2.9), with the boundary conditions,

$$q_c(0) = q, \qquad q_c(T) = q'$$

Now let us consider the action given by equation (2.6) with Hamiltonian given by (2.7). We denote this action at the critical point by the notation,

$$\tilde{S}_{\tilde{\mathbf{q}}_{\mathbf{c}}(t)}(q, q') = \tilde{S}[\tilde{\mathbf{q}}_{\mathbf{c}}(t)]$$

The left hand side of the above emphasizes the dependence of the action on the boundary conditions given above. Clearly $\tilde{S}[\tilde{\mathbf{q}}_{\mathbf{c}}(t)] = S[q_c(t)]$. A quick computation yields,

$$\frac{\partial q_c(T)}{\partial p} = \left(\frac{\partial \tilde{S}_{\tilde{\gamma}_c}(q, q')}{\partial q \partial q'}\right)^{-1}$$

Inserting the above equality into (2.12) gives an analogous formula in terms of the phase space formalism,

$$\left(\frac{\partial \tilde{S}_{\tilde{\gamma}_c}(q,q')}{\partial q \partial q'}\right)^{-1} = \frac{1}{2m}\det{}_\zeta A \tag{2.13}$$

Where A is again the operator given by equation (2.11).

2.4 A generalized Gelfand-Yaglom formula

We would like to amend the set up presented above in order to get a more generalized version of the Gelfand-Yaglom formula. To do so we will work in the Hamiltonian formalism and edit the action given in (2.6). To amend the action, we will define functions $f_1,\ f_2 :\ \mathbb{R}^2 \to \mathbb{R}$. Explicitly, f_1 is a function of the initial position $q = q(0)$ and a parameter b_1, while f_2 is a function of the final position $q' = q(T)$ and a parameter b_2. These functions define Lagrangian boundary conditions on the phase space. Do not confuse Lagrangian boundary conditions with the Lagrangian introduced in section 2.1.1. The generalized action functional can be written as,

$$\tilde{S}[\tilde{\mathbf{q}}_\mathbf{c}(t)] = \int_0^T \Big(p(t)\dot{q}(t) - H\big(p(t), q(t)\big)\Big)\, dt + f_1(q, b_1) - f_2(q', b_2) \tag{2.14}$$

We assume $\mathbb{R}^2$ has the standard symplectic structure with coordinates (p, q) and symplectic form $\omega = dp \wedge dq$. For now we will suppose $H\big(p(t), q(t)\big)$ is an arbitrary Hamiltonian that is at least twice differentiable in both variables. The critical points of the above generalized action functional are solutions to the boundary problem,

$$\dot{p}(t) = -\frac{\partial H}{\partial q(t)}\big(p(t), q(t)\big) \qquad \dot{q}(t) = \frac{\partial H}{\partial p(t)}\big(p(t), q(t)\big)$$

where

$$p(0) = \frac{\partial f_1}{\partial q} \qquad p(T) = \frac{\partial f_2}{\partial q'} \tag{2.15}$$

Thus critical points are flow lines of the Hamiltonian vector field generated by H, connecting the following two Lagrangian submanifolds

$$\mathcal{L}_1 = \left\{(p, q) \mid p = \frac{\partial f_1}{\partial q}(q, b_1)\right\}$$

$$\mathcal{L}_2 = \left\{(p, q') \mid p = \frac{\partial f_2}{\partial q'}(q', b_2)\right\}$$

in time T. The second variation of the action in (2.14) near the classical trajectory defines a first order differential operator $\tilde{A}$,

$$\delta^2 \tilde{S}[\tilde{\mathbf{q}}_\mathbf{c}(t)] = \int_0^T (\delta p,\ \delta q)\tilde{A}\begin{pmatrix}\delta p\\ \delta q\end{pmatrix}\ dt$$

where $\tilde{A}$ is defined explicitly as,

$$\tilde{A} = \begin{pmatrix} -\frac{\partial^2 H}{\partial p(t)^2}(p_c(t), q_c(t)) & \frac{d}{dt} - \frac{\partial^2 H}{\partial q(t)\partial p(t)}(p_c(t), q_c(t)) \\ -\frac{d}{dt} - \frac{\partial^2 H}{\partial q(t)\partial p(t)}(p_c(t), q_c(t)) & -\frac{\partial^2 H}{\partial q(t)^2}(p_c(t), q_c(t)) \end{pmatrix} \tag{2.16}$$

with boundary conditions,

$$x_2(0) = \frac{\partial^2 f_1}{\partial q^2}(q, b_1)x_1(0) \qquad x_2(T) = \frac{\partial^2 f_2}{\partial q'^2}(q', b_2)x_1(T) \tag{2.17}$$

where $\tilde{A}$ acts on the transpose of the vector $(x_1(t)\ x_2(t))$. The boundary conditions above translate to the mixed boundary conditions when considering the second order differential operator A. Explicitly, if A acts on the function $y(t)$ we can express the mixed boundary conditions as,

$$y'(0) = \frac{1}{m}\frac{\partial^2 f_1}{\partial q^2}(q, b_1)y(0) \qquad y'(T) = \frac{1}{m}\frac{\partial^2 f_2}{\partial q'^2}(q', b_2)y(T) \tag{2.18}$$

We desire a Gelfand-Yaglom formula that is analogous to equation (2.13) which uses the operator $\tilde{A}$ and the action given in (2.14), however when computing the ζ-regularized determinant of a first order operator the result depends on choosing a spectral cut in the plane and thus causes ambiguity.

Here we introduce an alternative regularization for the determinant of the operator $\tilde{A}$, which we refer to as the lattice-regularization. We compare this proposed regularization to the ζ-regularization with the goal of showing that they are agreeable. Moreover, computation of the lattice-regularization is simply a problem in matrix determinants and limits. To define the lattice-regularization, we first need to set up a discretized system.

2.5 A Discretized Generalized Gelfand-Yaglom Formula

Discretized Quantum Mechanics System

In this section, we will develop a discretized version of the usual quantum mechanics system. In this discrete setting, all determinants will be finite. This allows us to compute the following with ease: a generalized Gelfand-Yaglom formula in the Hamiltonian formalism, and a relationship between the determinants of the discretized versions of the operators A and $\tilde{A}$. Later, in section 2.6, we will consider how these results behave in the continuum limit, thus defining an alternative regularization for the determinants of A and $\tilde{A}$.

First we discretize any given path in $\mathbb{R}^n$, $\tilde{\mathbf{q}}(t) = \big(\vec{q}(t), \vec{p}(t)\big) :\ [0, T] \to \mathbb{R}^{2n}$, into N po-

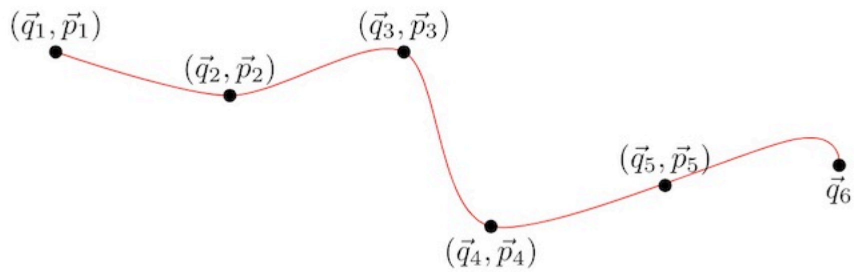

Figure 2.1: A discretization of a path into $N = 6$ position vectors and $N-1 = 5$ momentum vectors.

sition and $N-1$ momentum vectors as shown in figure 2.1, where $\vec{q}_i = \vec{q}\big((i-1)\cdot\epsilon\big)$ and $\vec{p}_i = \vec{p}\big((i-1)\cdot\epsilon\big)$ and $\epsilon = \frac{T}{N}$. From the above discretization and the action given in equation (2.14), we propose the following discrete action functional

$$\tilde{S}_d[\tilde{\mathbf{q}}_d(t)] = \sum_{i=1}^{N-1} \vec{p}_i(\vec{q}_{i+1} - \vec{q}_i) - \sum_{i=1}^{N-1} H(\vec{p}_i, \vec{q}_i) - f_2(\vec{q}_N, \vec{b}_2) + f_1(\vec{q}_1, \vec{b}_1) \tag{2.19}$$

where f_1 and f_2 are the same functions appearing in equation (2.14). We will only consider discrete Hamiltonians that arise from twice differentiable continuous Hamiltonians. Note that $\vec{q}_1 = \vec{q}(0) = q$ and $\vec{q}_N = \vec{q}(T) = q'$ are exactly what appears in the continuous statement of the action. From the above we derive a discrete version of Hamilton's equations,

$$\vec{q}_{i+1} - \vec{q}_i - \frac{\partial H}{\partial \vec{p}_i}(\vec{p}_i, \vec{q}_i) = 0 \quad i = 1, \ldots, N-1 \tag{2.20}$$

$$\vec{p}_i - \vec{p}_{i-1} + \frac{\partial H}{\partial \vec{q}_i}(\vec{p}_i, \vec{q}_i) = 0 \quad i = 2, \ldots, N-1 \tag{2.21}$$

and the boundary conditions,

$$\frac{\partial f_1}{\partial \vec{q}_1} = \vec{p}_1 + \frac{\partial H}{\partial \vec{q}_1}(\vec{p}_1, \vec{q}_1) \tag{2.22}$$

$$\frac{\partial f_2}{\partial \vec{q}_N} = \vec{p}_{N-1} \tag{2.23}$$

which agree with the conditions from (2.15) in the continuum limit. The discretized path, $\tilde{\mathbf{q}}_{d,c} = \{\vec{p}_1, \ldots, \vec{p}_{N-1}, \vec{q}_1, \ldots, \vec{q}_N\}$, that satisfies equations (2.20)-(2.23) will be known as the (discrete) critical point or classical path.

When we take the second variation of the discretized action functional we obtain a matrix operator which acts on the vector $\delta\tilde{\mathbf{q}}_{d,c}$ in the following manner,

$$\delta^2 S_d[\tilde{\mathbf{q}}_{d,c}] = \delta\tilde{\mathbf{q}}_{d,c}\tilde{A}_N(\delta\tilde{\mathbf{q}}_{d,c})^T$$

The matrix $\tilde{A}_N$ is the discrete analog of the Hamilton-Jacobi operator $\tilde{A}$ with N time intervals. To define $\tilde{A}_N$ explicitly, we should first note that it has a block form,

$$\tilde{A}_N = \begin{pmatrix} D_1 & D_2 \\ D_3 & D_4 \end{pmatrix} \tag{2.24}$$

In the one-dimensional case the block above can be written explicitly as,

$$(D_1)_{ij} = \begin{cases} -\dfrac{\partial^2 H}{\partial p_i \partial p_i} & \text{if } i = j \\ 0 & \text{if } i \neq j \end{cases}$$

$$(D_2)_{ij} = (D_3)_{ji} = \begin{cases} -1 - \dfrac{\partial^2 H}{\partial p_i \partial q_i} & \text{if } i = j \\ 1 & \text{if } i + 1 = j \\ 0 & \text{otherwise} \end{cases}$$

$$(D_4)_{ij} = \begin{cases} \dfrac{\partial^2 f_1}{\partial q_1 \partial q_1} - \dfrac{\partial^2 H}{\partial q_1 \partial q_1} & \text{if } i = j = 1 \\ -\dfrac{\partial^2 H}{\partial q_i \partial q_i} & \text{if } 2 \leq i = j \leq N-1 \\ -\dfrac{\partial^2 f_2}{\partial q_N \partial q_N} & \text{if } i = j = N \\ 0 & \text{if } i \neq j \end{cases}$$

where all derivatives are taken at the critical point. These matrices are immediately generalized to the n-dimensional case, where partial derivatives become $n \times n$ matrices of partial derivative and any constant is multiplied by the $n \times n$ identity matrix.

Discrete generalized Gelfand-Yaglom formula

We will restrict the following work to only include Hamiltonians that satisfy,

$$\det\left(\mathbb{I} + \frac{\partial^2 H}{\partial \vec{p}_i \partial \vec{q}_i}\right) \neq 0$$

and

$$\det\left(\frac{\partial^2 H}{\partial \vec{p}_i \partial \vec{p}_i}\right) \neq 0$$

for all $i = 1, \ldots, N-1$. From the above set up we derive a generalized GY formula. Note all determinant below are determinants of finite matrices.

Theorem 2.1. *The discrete action functional defined by* (2.19) *satisfies the generalized Gelfand-Yaglom formula*

$$\det\left(\frac{\partial^2 \tilde{S}_{d,\tilde{\mathbf{q}}_c}(b_1,b_2)}{\partial\vec{b}_1\partial\vec{b}_2}\right) = \prod_{i=1}^{N-1}\det\left(-\frac{\partial^2 H}{\partial\vec{p}_i\partial\vec{q}_i} - \mathbb{I}\right)\frac{\det\left(\dfrac{\partial^2 f_1}{\partial\vec{q}_1\partial\vec{b}_1}\right)\det\left(\dfrac{\partial^2 f_2}{\partial\vec{q}_N\partial\vec{b}_2}\right)}{\det\tilde{A}_N} \tag{2.25}$$

where $\tilde{S}_d[\tilde{\mathbf{q}}_c] = \tilde{S}_{d,\tilde{\mathbf{q}}_c}(b_1,b_2)$ *is the action at the classical path and* $\tilde{A}_N$ *is the Hamilton-Jacobi matrix operator.*

Proof. Throughout the proof we assume all $\vec{p}_i$ and $\vec{q}_i$ satisfy equations (2.20)-(2.23). To begin we directly compute the derivative of the action at the classical path with respect to $\vec{b}_1$,

$$\frac{\partial\tilde{S}_{d,\tilde{\mathbf{q}}_c}(b_1,b_2)}{\partial\vec{b}_1} = \sum_{i=1}^{N-1}\frac{\partial\vec{p}_i}{\partial\vec{b}_1}(\vec{q}_{i+1}-\vec{q}_i) + \sum_{i=1}^{N-1}\vec{p}_i\left(\frac{\partial\vec{q}_{i+1}}{\partial\vec{b}_1} - \frac{\partial\vec{q}_i}{\partial\vec{b}_1}\right) - \sum_{i=1}^{N-1}\frac{\partial H}{\partial\vec{p}_i}(\vec{p}_i,\vec{q}_i)\frac{\partial\vec{p}_i}{\partial\vec{b}_1}$$
$$+\sum_{i=1}^{N-1}\frac{\partial H}{\partial\vec{q}_i}(\vec{p}_1,\vec{q}_i)\frac{\partial\vec{q}_i}{\partial\vec{b}_1} - \frac{\partial f_2}{\partial\vec{q}_N}(\vec{q}_N,\vec{b}_2)\frac{\partial\vec{q}_N}{\partial\vec{b}_1} + \frac{\partial f_1}{\partial\vec{b}_1} + \frac{\partial f_1}{\partial\vec{q}_1}(\vec{q}_1,\vec{b}_1)\frac{\partial\vec{q}_1}{\partial\vec{b}_1}$$

Once we realize that the above derivative is taken at the classical path, many terms cancel. The first sum cancels with the third sum by equation (2.20) and if we rearrange the second sum to be,

$$\sum_{i=1}^{N-1}\vec{p}_i\left(\frac{\partial\vec{q}_{i+1}}{\partial\vec{b}_1} - \frac{\partial\vec{q}_i}{\partial\vec{b}_1}\right) = -\frac{\partial\vec{q}_1}{\partial\vec{b}_1}\vec{p}_1 - \sum_{i=2}^{N-1}\frac{\partial\vec{q}_i}{\partial\vec{b}_1}(\vec{p}_i - \vec{p}_{i-1}) + \frac{\partial\vec{q}_N}{\partial\vec{b}_1}\vec{p}_N$$

we see the above cancels out many of the other terms by (2.20), (2.22), and (2.23) and so we obtain,

$$\frac{\partial\tilde{S}_{d,\tilde{\mathbf{q}}_c}(b_1,b_2)}{\partial\vec{b}_1} = \frac{\partial f_1}{\partial\vec{b}_1} \tag{2.26}$$

Next taking the derivative with respect to $\vec{b}_2$ yields,

$$\frac{\partial^2\tilde{S}_{d,\tilde{\mathbf{q}}_c}(b_1,b_2)}{\partial\vec{b}_1\partial\vec{b}_2} = \left(\frac{\partial^2 f_1}{\partial\vec{q}_1\partial\vec{b}_1}\right)^T\left(\frac{\partial\vec{q}_1}{\partial\vec{b}_2}\right) \tag{2.27}$$

Note that the right hand side of equation (2.26) is truthfully,

$$\frac{\partial f_1}{\partial\vec{b}_1} = \frac{\partial f_1}{\partial\vec{b}_1}(\vec{q},\vec{b}_1)\bigg|_{\vec{q}=\vec{q}_1}$$

and thus it does not concern the dependence of $\vec{q}_1$ on $\vec{b}_1$. This will be the case whenever we write derivatives of f_1 or f_2 with respect to $\vec{b}_1$ or $\vec{b}_2$.

We would now like to replace $\partial\vec{q}_1/\partial\vec{b}_2$ in equation (2.27). To do so we will take the derivatives of equations (2.20)-(2.23) with respect to the Lagrangian parameter $\vec{b}_2$,

$$\frac{\partial\vec{q}_{i+1}}{\partial\vec{b}_2} - \frac{\partial\vec{q}_i}{\partial\vec{b}_2} - \frac{\partial^2 H}{\partial\vec{p}_i\partial\vec{p}_i}\frac{\partial\vec{p}_i}{\partial\vec{b}_2} + \frac{\partial^2 H}{\partial\vec{p}_i\partial\vec{q}_i}\frac{\partial\vec{q}_i}{\partial\vec{b}_2} = 0 \tag{2.28}$$

$$\frac{\partial\vec{p}_i}{\partial\vec{b}_2} - \frac{\partial\vec{p}_{i-1}}{\partial\vec{b}_2} + \frac{\partial^2 H}{\partial\vec{q}_i\partial\vec{q}_i}\frac{\partial\vec{q}_i}{\partial\vec{b}_2} + \frac{\partial^2 H}{\partial\vec{p}_i\partial\vec{q}_i}\frac{\partial\vec{p}_i}{\partial\vec{b}_2} = 0 \tag{2.29}$$

$$\frac{\partial^2 f_1}{\partial\vec{q}_1\partial\vec{q}_1}\frac{\partial\vec{q}_1}{\partial\vec{b}_2} = \frac{\partial\vec{p}_1}{\partial\vec{b}_2} + \frac{\partial^2 H}{\partial\vec{q}_1\partial\vec{q}_1}\frac{\partial\vec{q}_1}{\partial\vec{b}_2} + \frac{\partial^2 H}{\partial\vec{q}_1\partial\vec{p}_1}\frac{\partial\vec{p}_1}{\partial\vec{b}_2} \tag{2.30}$$

$$\frac{\partial^2 f_2}{\partial\vec{q}_N\partial\vec{b}_2} + \frac{\partial^2 f_2}{\partial\vec{q}_N\partial\vec{q}_N}\frac{\partial\vec{q}_N}{\partial\vec{b}_2} = \frac{\partial\vec{p}_{N-1}}{\partial\vec{b}_2} \tag{2.31}$$

First it will be useful to write equations (2.28) and (2.29) as the following recursive system of equations,

$$\begin{pmatrix} \dfrac{\partial\vec{q}_{i+1}}{\partial\vec{b}_2} \\ \dfrac{\partial\vec{q}_i}{\partial\vec{b}_2} \end{pmatrix} = U_i \begin{pmatrix} \dfrac{\partial\vec{q}_i}{\partial\vec{b}_2} \\ \dfrac{\partial\vec{q}_{i-1}}{\partial\vec{b}_2} \end{pmatrix} \tag{2.32}$$

where U_i is the $2n \times 2n$ block matrix,

$$U_i = \begin{pmatrix} \alpha_i & \beta_i \\ \mathbb{I} & 0 \end{pmatrix}$$

and the matrices α_i and β_i are given by the equations,

$$\alpha_i = \left(\mathbb{I} + \frac{\partial^2 H}{\partial\vec{p}_i\partial\vec{q}_i}\right) - \frac{\partial^2 H}{\partial\vec{p}_i\partial\vec{p}_i}\left(\mathbb{I} + \frac{\partial^2 H}{\partial\vec{p}_i\partial\vec{q}_i}\right)^{-1}\frac{\partial^2 H}{\partial\vec{q}_i\partial\vec{q}_i} + \frac{\partial^2 H}{\partial\vec{p}_i\partial\vec{p}_i}\left(\mathbb{I} + \frac{\partial^2 H}{\partial\vec{p}_i\partial\vec{q}_i}\right)^{-1}\left(\frac{\partial^2 H}{\partial\vec{p}_{i-1}\partial\vec{p}_{i-1}}\right)^{-1}$$

$$\beta_i = -\frac{\partial^2 H}{\partial\vec{p}_i\partial\vec{p}_i}\left(\mathbb{I} + \frac{\partial^2 H}{\partial\vec{p}_i\partial\vec{q}_i}\right)^{-1}\left(\frac{\partial^2 H}{\partial\vec{p}_{i-1}\partial\vec{p}_{i-1}}\right)^{-1}\left(\mathbb{I} + \frac{\partial^2 H}{\partial\vec{p}_{i-1}\partial\vec{q}_{i-1}}\right)$$

Note that there are no derivatives of $\vec{p}_i$ with respect to $\vec{b}_2$ in equation (2.32), as we can substitute equation (2.28) in equation (2.29) to eliminate it. Next we define the vector W_1, the initial vector of the recursive system, by,

$$W_1\frac{\partial\vec{q}_1}{\partial\vec{b}_2} = \begin{pmatrix} \dfrac{\partial\vec{q}_2}{\partial\vec{b}_2} \\ \dfrac{\partial\vec{q}_1}{\partial\vec{b}_2} \end{pmatrix}$$

and so explicitly we have,

$$W_1 = \begin{pmatrix} \left(\mathbb{I} + \dfrac{\partial^2 H}{\partial\vec{p}_1\partial\vec{q}_1}\right) + \dfrac{\partial^2 H}{\partial\vec{p}_1\partial\vec{p}_1}\left(\mathbb{I} + \dfrac{\partial^2 H}{\partial\vec{p}_1\partial\vec{q}_1}\right)^{-1}\left(\dfrac{\partial^2 f_1}{\partial\vec{q}_1\partial\vec{q}_1} - \dfrac{\partial^2 H}{\partial\vec{q}_1\partial\vec{q}_1}\right) \\ \mathbb{I} \end{pmatrix}$$

Combining W_1 with the system in equation (2.32) we have the useful relation,

$$\begin{pmatrix} \dfrac{\partial \vec{q}_N}{\partial \vec{b}_2} \\ \dfrac{\partial \vec{q}_{N-1}}{\partial \vec{b}_2} \end{pmatrix} = U_{N-1} \cdots U_2 W_1 \frac{\partial \vec{q}_1}{\partial \vec{b}_2}$$

Next we rewrite equation (2.31) by rearranging the terms and writing $\partial \vec{p}_{N-1}/\partial \vec{b}_2$ in terms of $\partial \vec{q}_{N-1}/\partial \vec{b}_2$ and $\partial \vec{q}_{N-2}/\partial \vec{b}_2$,

$$\frac{\partial^2 f_2}{\partial \vec{q}_N \partial \vec{b}_2} = W_2^T \begin{pmatrix} \dfrac{\partial \vec{q}_N}{\partial \vec{b}_2} \\ \dfrac{\partial \vec{q}_{N-1}}{\partial \vec{b}_2} \end{pmatrix}$$

Putting this all together we get the following convenient way of expressing equation (2.31),

$$\frac{\partial^2 f_2}{\partial \vec{q}_N \partial \vec{b}_2} = \left(W_2^T U_{N-1} \cdots U_2 W_1 \right) \frac{\partial \vec{q}_1}{\partial \vec{b}_2} \tag{2.33}$$

Observe in the one dimensional case ($n = 1$), the matrix product in (2.33) is a scalar. Generally, this matrix product gives an $n \times n$ matrix. Plugging equation (2.33) back into equation (2.27) yields,

$$\frac{\partial^2 \tilde{S}_{d,\tilde{\mathbf{q}}_c}(b_1, b_2)}{\partial \vec{b}_1 \partial \vec{b}_2} = \left(\frac{\partial^2 f_1}{\partial \vec{q}_1 \partial \vec{b}_1} \right)^T \left(W_2^T U_{N-1} \cdots U_2 W_1 \right)^{-1} \left(\frac{\partial^2 f_2}{\partial \vec{q}_N \partial \vec{b}_2} \right)$$

and taking the determinant gives,

$$\det \left(\frac{\partial^2 \tilde{S}_{d,\tilde{\mathbf{q}}_c}(b_1, b_2)}{\partial \vec{b}_1 \partial \vec{b}_2} \right) = \frac{\det \left(\dfrac{\partial^2 f_1}{\partial \vec{p}_1 \partial \vec{b}_1} \right) \det \left(\dfrac{\partial^2 f_2}{\partial \vec{p}_N \partial \vec{b}_2} \right)}{\det \left(W_2^T U_{N-1} \cdots U_2 W_1 \right)} \tag{2.34}$$

Now let's write the denominator of (2.34) in terms of the determinant of the Hamilton-Jacobi matrix operator, $\tilde{A}_N$. To do so we will need the following technical lemma,

Lemma 2.1.1. *For the* $(2Nn - n) \times (2Nn - n)$ *Hamilton-Jacobi matrix* $\tilde{A}_N$*,*

$$\det \tilde{A}_N = (-1)^{Nn} \left[\prod_{i=1}^{N-1} \det \left(-\frac{\partial^2 H}{\partial \vec{p}_i \partial \vec{p}_i} \right) \right] \det \left(V_2^T T_{N-1} \cdots T_2 V_1 \right) \det \left(B_{N-1} \cdots B_1 \right) \tag{2.35}$$

Where we define the block matrices,

$$T_i = \begin{pmatrix} -B_i^{-1}E_i & -B_i^{-1}C_{i-1} \\ \mathbb{I} & 0 \end{pmatrix} \tag{2.36}$$

$$V_1 = \begin{pmatrix} -B_1^{-1}E_1 \\ \mathbb{I} \end{pmatrix} \tag{2.37}$$

$$V_2 = \begin{pmatrix} -E_N \\ -C_{N-1} \end{pmatrix} \tag{2.38}$$

and the $m \times m$ matrices,

$$E_i = \begin{cases} \frac{\partial^2 f_1}{\partial \vec{q}_1 \partial \vec{q}_1} - \frac{\partial^2 H}{\partial \vec{q}_1 \partial \vec{q}_1} + \left(\mathbb{I} + \frac{\partial^2 H}{\partial \vec{p}_1 \partial \vec{q}_1}\right)\left(\frac{\partial^2 H}{\partial \vec{q}_1 \partial \vec{q}_1}\right)^{-1}\left(\mathbb{I} + \frac{\partial^2 H}{\partial \vec{p}_1 \partial \vec{q}_1}\right) & i = 1 \\ -\frac{\partial^2 H}{\partial \vec{q}_i \partial \vec{q}_i} + \left(\frac{\partial^2 H}{\partial \vec{p}_{i-1} \partial \vec{p}_{i-1}}\right)^{-1} & \\ \qquad + \left(\mathbb{I} + \frac{\partial^2 H}{\partial \vec{p}_i \partial \vec{q}_i}\right)\left(\frac{\partial^2 H}{\partial \vec{p}_i \partial \vec{p}_i}\right)^{-1}\left(\mathbb{I} + \frac{\partial^2 H}{\partial \vec{p}_i \partial \vec{q}_i}\right) & 2 \leq i \leq N-1 \\ -\frac{\partial^2 f_2}{\partial \vec{q}_N \partial \vec{q}_N} + \left(\frac{\partial^2 H}{\partial \vec{p}_{N-1} \partial \vec{p}_{N-1}}\right)^{-1} & i = N \end{cases} \tag{2.39}$$

$$B_i = \left(\mathbb{I} + \frac{\partial^2 H}{\partial \vec{p}_i \partial \vec{q}_i}\right)\left(\frac{\partial^2 H}{\partial \vec{p}_i \partial \vec{p}_i}\right)^{-1} \tag{2.40}$$

$$C_i = \left(\frac{\partial^2 H}{\partial \vec{p}_i \partial \vec{p}_i}\right)^{-1}\left(\mathbb{I} + \frac{\partial^2 H}{\partial \vec{p}_i \partial \vec{q}_i}\right) \tag{2.41}$$

The above lemma is proved in Appendix A and depends largely on a result in [20]. An easy computation reveals the relationships,

$$V_i = \begin{pmatrix} -\mathbb{I} & 0 \\ 0 & \mathbb{I} \end{pmatrix} W_i$$

$$T_i = \begin{pmatrix} -\mathbb{I} & 0 \\ 0 & \mathbb{I} \end{pmatrix} U_i \begin{pmatrix} \mathbb{I} & 0 \\ 0 & -\mathbb{I} \end{pmatrix}$$

and so we can rewrite equation (2.35) in terms of the W and U matrices,

$$\det \tilde{A}_N = \left[\prod_{i=1}^{N-1} \det\left(-\frac{\partial^2 H}{\partial \vec{p}_i \partial \vec{p}_i}\right) \det B_i\right] \det\left(W_2^T U_{N-1} \cdots U_2 W_1\right) \tag{2.42}$$

Using the definition of the B_i matrices and plugging the above into equation (2.34) we obtain,

$$\det\left(\frac{\partial^2 \tilde{S}_{\tilde{\mathbf{q}}_c}(b_1,b_2)}{\partial\vec{b}_1\partial\vec{b}_2}\right) = \left[\prod_{i=1}^{N-1}\det\left(-\mathbb{I}-\frac{\partial^2 H}{\partial\vec{p}_i\partial\vec{q}_i}\right)\right]\frac{\det\left(\frac{\partial^2 f_1}{\partial\vec{q}_1\partial\vec{b}_1}\right)\det\left(\frac{\partial^2 f_2}{\partial\vec{q}_N\partial\vec{b}_2}\right)}{\det\tilde{A}_N}$$

which is precisely the statement from Theorem 2.1. □

We will be particularly interested in the case where $H(p_i,q_i)=\frac{1}{2m}p_i^2+V(q_i)$ where the statement from Theorem 2.1 simplifies to,

$$\det\left(\frac{\partial^2 \tilde{S}_{\tilde{\gamma}_c}(b_1,b_2)}{\partial\vec{b}_1\partial\vec{b}_2}\right) = (-1)^{n(N-1)}\frac{\det\left(\frac{\partial^2 f_1}{\partial\vec{q}_1\partial\vec{b}_1}\right)\det\left(\frac{\partial^2 f_2}{\partial\vec{q}_N\partial\vec{b}_2}\right)}{\det\tilde{A}_N}$$

Moreover, we will now assume N is odd, so the above formula becomes

$$\det\left(\frac{\partial^2 \tilde{S}_{\tilde{\mathbf{q}}_c}(b_1,b_2)}{\partial\vec{b}_1\partial\vec{b}_2}\right) = \frac{\det\left(\frac{\partial^2 f_1}{\partial\vec{q}_1\partial\vec{b}_1}\right)\det\left(\frac{\partial^2 f_2}{\partial\vec{q}_N\partial\vec{b}_2}\right)}{\det\tilde{A}_N} \tag{2.43}$$

A Discretization of A

Now we will consider the operator A with boundary conditions given by equation (2.18). We will define a discretized version of A which we will refer to as A_N and compare the determinant of this finite operator with the determinant of the aforementioned discrete operator, $\tilde{A}_N$. This will set us up to further analyze these operators in section 2.6.

Let us begin by defining a discrete analog of the operator A in the one-dimensional case. This definition is under the assumption $\epsilon=1$ (as was the case when we defined $\tilde{A}_N$). In section 2.6, we will expand this definition for arbitrary ϵ in order to consider the convergence of the operator (and its determinant).

$$(A_N)_{jk} = \begin{cases} -1 & \text{if } j=k+1 \text{ or } k=j+1 \\ \frac{a_1}{m}+1-\frac{1}{m}V_j'' & \text{if } j=k=1 \\ 2-\frac{1}{m}V_j'' & \text{if } j=k \text{ and } 2\le j\le N-1 \\ -\frac{a_2}{m}+1 & \text{if } i=k=1 \\ 0 & \text{otherwise} \end{cases} \tag{2.44}$$

where $V_j''=V''(q_j)$ and

$$a_1=\frac{\partial^2 f_1}{\partial q^2}(q,b_1) \qquad a_2=\frac{\partial^2 f_2}{\partial q'^2}(q',b_2)$$

With this in mind we state the following theorem,

Theorem 2.2. *Consider the discrete operators A_N and $\tilde{A}_N$, along with the corresponding Hamiltonian is $H(p_i, q_i) = \frac{1}{2m}p_i^2 + V(q_i)$. Their determinants are related by the following formula for all $N \geq 2$.*

$$\det \tilde{A}_N = (-1)^{N-1} m \det A_N \tag{2.45}$$

Proof. The result follows immediately from the fact that, $\det \tilde{A}_N = \det D_1 \det(D_4 - D_3 D_1^{-1} D_2)$ and the observation that, $D_4 - D_3 D_1^{-1} D_2 = m \cdot A_N$ for all N and all twice differentiable function $V(q_i)$. □

An immediate consequence of the above theorem is the following corollary,

Corollary 2.2.1. *For the discrete operator A_N with associated Hamiltonian $H(p_i, q_i) = \frac{1}{2m}p_i^2 + V(q_i)$ and mixed boundary conditions from (2.18), the following discrete generalized Gelfand-Yaglom formula holds*

$$\det(A_N) = \frac{1}{m} \frac{\dfrac{\partial^2 f_1}{\partial b_1 \partial q_1} \dfrac{\partial^2 f_2}{\partial b_2 \partial q_N}}{\dfrac{\partial^2 S_{d,\tilde{\mathbf{q}}_c}(b_1, b_2)}{\partial b_1 \partial b_2}}$$

2.6 Asymptotics and a Lattice Regularization

In this section we will show that the discrete operators $\tilde{A}_N$ and A_N converge to their continuous counterparts in the continuum limit. Moreover, we will show that we can make sense of the determinants of the A_N and $\tilde{A}_N$ in this limit. This will lead us to define a lattice regularization in regards to the determinants of these operators.

As in section 2.5, we will be considering the one-dimensional case where N is odd and $H(p_i, q_i) = \frac{1}{2m}p_i^2 + V(q_i)$. We will also employ the following notation as short hand,

$$a_1 = \frac{\partial^2 f_1}{\partial q_1 \partial q_1}(q_1, b_1) \qquad a_2 = \frac{\partial^2 f_2}{\partial q_N \partial q_N}(q_N, b_2) \tag{2.46}$$

Convergence of $\tilde{A}_N$

Here we consider the operator $\tilde{A}$ given by equation (2.16). We denote the associated twice differentiable, continuous Hamiltonian by $\mathcal{H}\big(p(t), q(t)\big)$. The operator $\tilde{A}$ acts on the domain,

$$D(\tilde{A}) = \left\{ \begin{pmatrix} x_1(t) \\ x_2(t) \end{pmatrix} \;\middle|\; x_1, x_2 \in C^1\big([0,T]\big) \text{ and } x_1(0) = a_1 x_2(0),\; x_1(T) = a_2 x_2(T) \right\}$$

where the last two conditions are just the boundary conditions stated in (2.17).

The associated discrete operator, $\tilde{A}_N$ arises from the discrete Hamilitonian $H(p_i, q_i) = \epsilon \cdot \mathcal{H}\big(p(t_i), q(t_i)\big)$. Recall that the parameter $\epsilon = \frac{T}{N-1}$ splits the interval $[0, T]$ into N equally spaced time points. The domain of $\tilde{A}_N$ is,

$$D(\tilde{A}_N) = \left\{ \begin{pmatrix} x_1(t_1) \\ \vdots \\ x_1(t_{N-1}) \\ x_2(t_1) \\ \vdots \\ x_2(t_N) \end{pmatrix} : \begin{pmatrix} x_1(t) \\ x_2(t) \end{pmatrix} \in D\big(\tilde{A}\big) \right\}$$

Theorem 2.3. *The discrete operator $\tilde{A}_N$ converges weakly to the operator $\tilde{A}$ as $N \to \infty$ for any twice differentiable Hamiltonian $\mathcal{H}\big(p(t), q(t)\big)$.*

Proof. Let's first define the vectors $X, Y \in D\big(\tilde{A}\big)$ as

$$X = \begin{pmatrix} x_1(t) \\ x_2(t) \end{pmatrix}, \quad Y = \begin{pmatrix} y_1(t) \\ y_2(t) \end{pmatrix}$$

and the corresponding vectors X_N, $Y_N \in D(\tilde{A}_N)$ as,

$$X_N = \begin{pmatrix} x_1(t_1) \\ \vdots \\ x_1(t_{N-1}) \\ x_2(t_1) \\ \vdots \\ x_2(t_N) \end{pmatrix}, \quad Y_N = \begin{pmatrix} y_1(t_1) \\ \vdots \\ y_1(t_{N-1}) \\ y_2(t_1) \\ \vdots \\ y_2(t_N) \end{pmatrix}$$

To show weak convergence, we will show that

$$\lim_{N\to\infty} Y_N^T \mathcal{D}_N X_N = \int_0^T Y^T \tilde{A} X \, dt \tag{2.47}$$

We compute that,

$$\begin{aligned} Y_N^T \tilde{A}_N X_N = &- \sum_{i=1}^{N-1} \epsilon y_1(t_i) \frac{\partial^2 \mathcal{H}}{\partial p^2} x_1(t_i) + \sum_{i=1}^{N-1} \epsilon y_1(t_i) \left[\left(\frac{x_2(t_{i+1}) - x_2(t_i)}{\epsilon} \right) - \frac{\partial^2 \mathcal{H}}{\partial p \partial q} x_2(t_i) \right] \\ &- \sum_{i=1}^{N-1} \epsilon y_2(t_i) \frac{\partial^2 \mathcal{H}}{\partial q^2} x_2(t_i) - \sum_{i=1}^{N-1} \epsilon y_2(t_i) \frac{\partial^2 \mathcal{H}}{\partial p \partial q} x_1(t_i) - \sum_{i=1}^{N-2} \epsilon y_2(t_i) \left(\frac{x_1(t_{i+1}) - x_1(t_i)}{\epsilon} \right) \\ &- \big(x_1(t_1) - a_1 x_2(t_1)\big) + \big(x_1(t_{N-1}) - a_2 x_2(t_N)\big) \end{aligned}$$

Now taking the limit gives,

$$\begin{aligned}\lim_{N\to\infty} Y_N^T \tilde{A}_N X_N = &-\int_0^T y_1(t)\frac{\partial^2\mathcal{H}}{\partial p^2}x_1(t)dt + \int_0^T y_1(t)\left[x_2'(t) - \frac{\partial^2\mathcal{H}}{\partial p\partial q}x_2(t)\right]dt \\ &-\int_0^T y_2(t)\left[x_1'(t) + \frac{\partial^2\mathcal{H}}{\partial p\partial q}\right]dt - \int_0^T y_2(t)\frac{\partial^2\mathcal{H}}{\partial p^2}x_2(t)dt \\ &-\big(x_1(0) - a_1x_2(0)\big) + \big(x1(T) - a_2x_2(T)\big) \\ \lim_{N\to\infty} Y_N^T \tilde{A}_N X_N = &\int_0^T Y^T\tilde{A}Xdt - \big(x_1(0) - a_1x_2(0)\big) + \big(x_1(T) - a_2x_2(T)\big)\end{aligned}$$

The boundary terms are zero for all $X \in D\big(\tilde{A}\big)$ and so the above statement is exactly equation (2.47). □

Specifically restricting to the case where $\mathcal{H}\big(p(t), q(t)\big) = \frac{1}{2m}p(t)^2 + V\big(q(t)\big)$, we can take the limit of equation (2.43). Under the convention that N is odd this gives,

$$\lim_{N\to\infty} \det \tilde{A}_N = \frac{\dfrac{\partial^2 f_1}{\partial q\partial b_1}\dfrac{\partial^2 f_2}{\partial q'\partial b_2}}{\dfrac{\partial^2 \tilde{S}_{\tilde{\mathbf{q}}_{\mathbf{c}}}(b_1, b_2)}{\partial b_1\partial b_2}} \tag{2.48}$$

The right hand side of the above equation is well-defined and finite, therefore the limit on the left hand side is also well-defined and finite. We will use this limit later in section 2.6 to define lattice-regularization. Note that the convergence of this limit is no longer clear in the case of a Hamiltonian with mixed terms.

Convergence of A_N

We now return to the operator A from equation (2.11) and its finite counterpart A_N.

Theorem 2.4. *The operator A_N weakly converges to the operator A.*

Proof. We first must define the domains of the operators A and A_N. The operator A has the domain,

$$D(A) = \big\{y(t) \in C^2([0,T]) \mid y'(0) = a_1 \cdot y(0),\ y'(T) = a_2 \cdot y(T)\big\}$$

where the mixed boundary conditions match the boundary conditions on $\tilde{A}$ given by equation (2.17). The domain of the operator A_N is,

$$D(A_N) = \left\{ \begin{pmatrix} y(t_1) \\ \vdots \\ y(t_N) \end{pmatrix} \middle|\ y(t) \in D(A) \right\}$$

Previously when defining A_N we used the convention $\epsilon = 1$, so we first need to reinsert epsilons into A_N where appropriate. For the case of $N = 4$ and $A = -\frac{d^2}{dt^2} - \frac{1}{m}V''(q_c(t))$ the operator A_N is,

$$A_4 = \begin{pmatrix} \frac{a_1}{m} + \frac{1}{\epsilon} - \frac{\epsilon}{m}V''\big(q_c(t_1)\big) & -\frac{1}{\epsilon} & 0 & 0 \\ -\frac{1}{\epsilon} & \frac{2}{\epsilon} - \frac{\epsilon}{m}V''\big(q(t_2)\big) & -\frac{1}{\epsilon} & 0 \\ 0 & -\frac{1}{\epsilon} & 2 - \frac{\epsilon}{m}V''\big(q(t_2)\big) & -\frac{1}{\epsilon} \\ 0 & 0 & -\frac{1}{\epsilon} & -\frac{a_2}{m} + \frac{1}{\epsilon} \end{pmatrix}$$

The above is easily generalized for arbitrary N. Let $x(t), y(t) \in D(A)$ and let $X_N, Y_N \in D(A_N)$ be their corresponding discrete versions. We will show that,

$$\lim_{N\to\infty} Y_N^T A_N X_N = \int_0^T y(t)Ax(t)dt \tag{2.49}$$

First we compute,

$$\begin{aligned} Y_N A_N X_N = y(t_1)\left(-\frac{x(t_2)-x(t_1)}{\epsilon} + \frac{a_1}{m}x(t_1)\right) - \sum_{i=1}^{N-1} y(t_i)\frac{\epsilon}{m}V''\big(q_c(t_i)\big)x(t_i) \\ - \sum_{i=2}^{N-1}\epsilon y(t_i)\left(\frac{x(t_{i+1}) - 2x(t_i) + x(t_{i-1})}{\epsilon^2}\right) + y(t_N)\left(\frac{x(t_N)-x(t_{N-1})}{\epsilon} - \frac{a_2}{m}x(t_N)\right) \end{aligned}$$

Taking the limit yields,

$$\begin{aligned} \lim_{N\to\infty} Y_N A_N X_N &= y(0)\left(x'(0) + \frac{a_1}{m}x(0)\right) - \int_0^T y(t)\frac{1}{m}V''\big(q_c(t)\big)x(t)dt \\ &\quad - \int_0^T y(t)x''(t)dt + y(T)\left(x'(T) - \frac{a_2}{m}x(T)\right) \\ \lim_{N\to\infty} &= \int_0^T y(t)Ax(t)dt + y(0)\left(x'(0) + \frac{a_1}{m}x(0)\right) + y(T)\left(x'(T) - \frac{a_2}{m}x(T)\right) \end{aligned}$$

The boundary terms are zero for all $x(t) \in D(A)$ and so the above statement is exactly equation (2.49). □

Again, lut us restrict to the case of $\mathcal{H}\big(p(t), q(t)\big) = \frac{1}{2m}p(t)^2 + V\big(q(t)\big)$. After generalizing for arbitrary ϵ, equation (2.45) becomes

$$\det \tilde{A}_N = m\epsilon^{N-1} \det A_N \tag{2.50}$$

where we must now be cognisant of the epsilons in A_N and $\tilde{A}_N$. Plugging this into (2.43), in order to get something convergent we must take a regularized determinant where we throw out the factor of ϵ^{-N+1},

$$\lim_{N\to\infty} \det{}' A_N = \frac{\dfrac{\partial^2 f_1}{\partial q \partial b_1} \dfrac{\partial^2 f_2}{\partial q' \partial b_2}}{m \dfrac{\partial^2 \tilde{S}_{\tilde{\mathbf{q}}_c}(b_1, b_2)}{\partial b_1 \partial b_2}}$$

where the apostrophe indicates that we have removed the epsilons. Again, the right hand side above is well-defined and finite.

It should be noted that for arbitrary ϵ, the determinant of $\tilde{A}_N$ converges plainly, however the determinant of A_N does not. In the latter case we need to remove the divergence. This might motivate the Hamilton-Jacobi operator being a more natural choice over Laplacian-type operators.

Defining a Lattice Regularization

As show in sections 2.6 and 2.6, one can make meaning out of the limits $\lim_{N\to\infty} \det \tilde{A}_N$ and $\lim_{N\to\infty} \det A_N$ in the case where $H(p_i, q_i) = \frac{p_i^2}{2m} + V(q_i)$. The following definition is a natural consequence,

Definition 2.1. *We define the lattice regularized determinants of A and $\tilde{A}$ by,*

$$\det{}_{reg}(A) = \lim_{N\to\infty} \det{}'(A_N) \tag{2.51}$$

$$\det{}_{reg}(\tilde{A}) = \lim_{N\to\infty} \det\left(\tilde{A}_N\right) \tag{2.52}$$

Tautologically, we have the identity

$$\det{}_{\text{reg}}\left(\tilde{A}\right) = m \det{}_{\text{reg}}\left(A\right) \tag{2.53}$$

The above definitions accompanied with equation (2.48) give use a generalized GY formula for the lattice regularized determinant of the operator A,

$$\det{}_{\text{reg}} A = \frac{\dfrac{\partial^2 f_1}{\partial q \partial b_1} \dfrac{\partial^2 f_2}{\partial q' \partial b_2}}{m \dfrac{\partial^2 \tilde{S}_{\tilde{\mathbf{q}}_c}(b_1, b_2)}{\partial b_1 \partial b_2}} \tag{2.54}$$

2.7 A Generalized Gelfand-Yaglom Formula for the Zeta Regularization

In this section, we will first derive a Gelfand Yaglom formula for the ζ-regularized determinant of the second order operator $L = -\frac{d^2}{dt^2} + u(t)$ equipped with mixed boundary conditions. While this formula is not new, it was first derived more generally in [4], we will specifically relate it to the operator A with relevant boundary conditions. Moreover, by restating these results we will be able to make a comparison to the formula in equation (2.54).

Derivation of a generalized GY formula for the configuration space

We will start by letting $u(t) \in C^1([0,T], \mathbb{R})$, then consider the differential operator,

$$L = -\frac{d^2}{dt^2} + u(t) \tag{2.55}$$

on the interval $t \in [0,T]$ with the domain,

$$D(L) = \left\{ y(t) \in W^{2,2}(0,T) \ : \ \frac{dy(0)}{dt} = \frac{a_1}{m} y(0), \ \frac{dy(T)}{dt} = \frac{a_2}{m} y(T) \right\} \tag{2.56}$$

where $W^{2,2}(0,T)$ denotes the Sobelov space and a_1, a_2 and m are nonzero constants named suggestively. We will also need to consider the second order differential equation,

$$-\ddot{y} + u(t) y = \lambda y \tag{2.57}$$

with parameter λ and where a dot denotes the derivative with respect to t. Let $y_1(t, \lambda)$ and $y_2(t, \lambda)$ denote two solutions of (2.57) with the following boundary conditions,

$$y_1(0, \lambda) = 1, \ \dot{y}_1(0, \lambda) = \frac{a_1}{m} \tag{2.58}$$

$$y_2(T, \lambda) = 1, \ \dot{y}_2(T, \lambda) = \frac{a_2}{m} \tag{2.59}$$

We are now able to state the following result, which is a specialization of a theorem first proved in [4],

Theorem 2.5 (Burghelea, Friedlander, Kappeler [4])**.** *Let $y_1(t) = y_1(t, 0)$ be the solution given above. Then,*

$$\det{}_{\zeta} L = 2 \left(\dot{y}_1(T) - \frac{a_2}{m} y_1(T) \right) \tag{2.60}$$

where L is the differential operator defined by equations (2.55) *and* (2.56).

Proof. Let's start by taking a closer look at the differential operator, L. The operator, L, is a regular Sturm-Liouville operator and thus has a discrete spectrum with simple eigenvalues, $\lambda_1 < \lambda_2 < \cdots < \lambda_n < \cdots$, accumulating to infinity. Moreover, the eigenvalues exhibit the following asymptotic behavior,

$$\lambda_n = \frac{\pi^2 n^2}{T^2} + O(1)$$

The details of this can be found in [18] among other texts. It then follows that the resolvent of L, $R_\lambda = (L - \lambda I)^{-1}$, is a trace class operator. So we can write the useful relation,

$$\frac{d}{d\lambda} \log \det{}_\zeta (L - \lambda I) = -\text{Tr } R_\lambda \tag{2.61}$$

where any zero eigenvalues are first removed. Using variation of parameter on the inhomogeneous equation,

$$-\ddot{y} + u(t)y = \lambda y + f(x), \quad \lambda \neq \lambda_n$$

we get the solution,

$$y(x) = \int_0^T R_\lambda(x, \xi) f(\xi) d\xi$$

where

$$R_\lambda(x, \xi) = \begin{cases} \dfrac{y_1(x,\lambda) y_2(\xi,\lambda)}{W(y_1, y_2)} & \text{if } x \leq \xi \\ \dfrac{y_1(\xi,\lambda) y_2(x,\lambda)}{W(y_1, y_2)} & \text{if } x \geq \xi \end{cases} \tag{2.62}$$

is the resolvent of L. In the above, $W(y_1, y_2)$ denotes the Wronskian of the two solutions. We manipulate the right hand side of equation (2.61) as follows,

$$\begin{aligned} -\text{Tr } R_\lambda &= -\int_0^T R_\lambda(x, x) dx \\ &= \frac{-1}{W(y_1, y_2)} \int_0^T y_1(x,\lambda) y_2(x,\lambda) dx \\ &= \frac{1}{W(y_1, y_2)} \left[W\left(\frac{dy_1}{d\lambda}, y_2 \right) \right]_0^T \\ &= \frac{d}{d\lambda} \log \left[\frac{a_2}{m} y_1(T,\lambda) - \dot{y}_1(T,\lambda) \right] \end{aligned}$$

Plugging the above back into (2.61) gives,

$$\det{}_\zeta (L - \lambda I) = C \cdot \left[\frac{a_2}{m} y_1(T,\lambda) - \dot{y}_1(T,\lambda) \right] \tag{2.63}$$

where C is some constant. To compute C, we will let $\lambda = -\mu$ and consider the asymptotics of both sides of the equation as $\mu \to \infty$. To start let's compute the asymptotics of $\det(L + \mu I)$.

We write the ζ-function of $L+\mu I$ using the contour integral method described in [17],

$$\zeta_{L+\mu I}(s) = \frac{1}{2\pi i}\int_\gamma dx x^{-s}\frac{d}{dx}\log\omega(x-\mu) \tag{2.64}$$

where γ is the curve encircling all the eigenvalues of $L+\mu I$ and $\omega(x-\mu)$ is a smooth function of x with zero at the eigenvalues of the operator $L+\mu I$. Let $\sqrt{x}=\sigma+ri$, then

$$\omega(x) = -\sqrt{x}\sin\left(T\sqrt{x}\right) + O\left(e^{|r|T}\right) \tag{2.65}$$

The full computation of these asymptotics can be found in [8]. Next we deform the contour and we rewrite the integral as,

$$\zeta_{L+\mu I}(s) = \frac{\sin(\pi s)}{\pi}\int_0^\infty dx x^{-s}\frac{d}{dx}\log\omega(-x-\mu) \tag{2.66}$$

The above integral converges near 0 for $s=0$, however the integral does not converge near infinity for $s=0$. To analytically continue the function we write,

$$\zeta_{L+\mu I}(s) = \zeta_1(s)+\zeta_2(s)+\zeta_3(s)$$

where

$$\begin{aligned}
\zeta_1(s) &= \frac{\sin(\pi s)}{\pi}\int_0^1 dx x^{-s}\frac{d}{dx}\log\omega(-x-\mu)\\
\zeta_2(s) &= \frac{\sin(\pi s)}{\pi}\int_1^\infty dx x^{-s}\frac{d}{dx}\log\left(\omega(-x-\mu)\frac{2}{\sqrt{x}}e^{-T\sqrt{x}}\right)\\
\zeta_3(s) &= \frac{\sin(\pi s)}{\pi}\int_1^\infty dx x^{-s}\frac{d}{dx}\log\left(\frac{1}{2}\sqrt{x}e^{T\sqrt{x}}\right)
\end{aligned}$$

The first two integrals converge for $s=0$ and we can easily analytically continue the third using the method described in [17]. Using the above we compute,

$$\zeta'_{L+\mu I}(0) = -\log 2w(-\mu)$$

and so the determinant is,

$$\det{}_\zeta(L+\mu I) = 2w(-\mu)$$

Asymptotically we can write,

$$\det{}_\zeta(L+\mu I) = 2\sqrt{\mu}\sinh\left(T\sqrt{\mu}\right) + O\left(e^{T\sqrt{\mu}}\right) \tag{2.67}$$

Now we will consider the right hand side of equation (2.63). Again, let $\sqrt{x}=\sigma+ri$. We will also let $k=\int_0^T u(t)dt$. The function $y_1(T,x)$ has the following asymptotic expansions [8],

$$y_1(T,x) = \cos(T\sqrt{x}) + \left(\frac{a_1}{m\sqrt{x}}+\frac{k}{2\sqrt{x}}\right)\sin(T\sqrt{x}) + O\left(\frac{1}{|x|}e^{T|r|}\right)$$

And so equation (2.63) becomes,

$$\det{}_\zeta(L+\mu I) = C \cdot \left[-\sqrt{\mu}\sinh(T\sqrt{\mu}) + O(e^{T\sqrt{\mu}})\right] \tag{2.68}$$

Comparing equations (2.67) and (2.68), we see that $C = -2$, so equation (2.63) becomes

$$\det{}_\zeta(L-\lambda I) = 2\left(\dot{y}_1(T,\lambda) - \frac{a_2}{m}y_1(T,\lambda)\right) \tag{2.69}$$

In particular, if we consider the case of $\lambda = 0$, we return the results from Theorem 2.5. □

Note that in the case where $a_1 = a_2 = 0$ we recover the case of Neumann boundary conditions. The case of Dirichlet boundary conditions cannot be extracted from the above theorem, however the result is well known [23]. Let us now relate the above formula to the quantum system described in section 2.4 with Lagrangian boundary conditions. First let,

$$u(t) = -\frac{1}{m}V''(q_c(t))$$

where $q_c(t)$ is the classical path. Note the classical path has the initial conditions,

$$q_c(0) = q, \quad \dot{q}_c(0) = \frac{1}{m}\frac{\partial f_1}{\partial q} \tag{2.70}$$

which leads us to the following lemma,

Lemma 2.5.1. *The function $y(t) = \frac{\partial q_c(t)}{\partial q}$ with boundary conditions,*

$$y(0) = 1 \quad \dot{y}(0) = \frac{a_1}{m}$$

satisfies the differential equation,

$$m\ddot{y}(t) = -V''(q_c(t))\,y(t)$$

The above lemma is a simple exercises in derivatives. The following corollary is an immediate result of Theorem 2.5 and Lemma 2.5.1.

Corollary 2.5.1. *For the operator A with domain given by* (2.56) *we have the generalized Gelfand-Yaglom formula,*

$$\det{}_\zeta A = 2\left(\frac{\partial \dot{q}_c(T)}{\partial q} - \frac{a_2}{m}\frac{\partial q_c(T)}{\partial q}\right)$$

where $q_c(t)$ is the classical path satisfying equations (2.5) *and* (2.70).

A generalized GY formula for the phase space and A

In this section, we will reformulate the prior corollary to be in terms of derivatives of the action functional stated in (2.14). We claim,

Theorem 2.6. *For the action given in equation* (2.14) *with a Hamiltonian of the form,* $H(p,q) = \frac{p^2}{2m} + V(q)$, *the following generalized Gelfand-Yaglom formula holds,*

$$\frac{\partial^2 \tilde{S}_{\tilde{\gamma}_c}(b_1, b_2)}{\partial b_1 \partial b_2} = 2\frac{\dfrac{\partial^2 f_1}{\partial q \partial b_1}\dfrac{\partial^2 f_2}{\partial q' \partial b_2}}{m \det{}_{\zeta} A} \tag{2.71}$$

Proof. Let's start by taking derivatives of the action at the critical value,

$$\frac{\partial^2 \tilde{S}_{\tilde{\gamma}_c}(b_1, b_2)}{\partial b_1 \partial b_2} = \frac{\partial^2 f_1}{\partial b_1 \partial q}\frac{\partial q}{\partial b_2} \tag{2.72}$$

Recall the second boundary condition from equation (2.15). Taking the derivative with respect to b_2 gives,

$$\frac{\partial^2 f_2}{\partial q' \partial b_2} + a_2 \cdot \frac{\partial q'}{\partial b_2} = \frac{\partial p'}{\partial b_2}$$

The above uses the notation $q(T) = q'$, $p(T) = p'$, and the shorthand given in equation (2.46). Let us rewrite the above, using relation $p(t) = m\dot{q}(t)$.

$$\frac{\partial^2 f_2}{\partial q' \partial b_2} = -a_2 \cdot \frac{\partial q'}{\partial q}\frac{\partial q}{\partial b_2} + m \cdot \frac{\partial \dot{q}'}{\partial q}\frac{\partial q}{\partial b_2}$$

Now let's use Corollary 2.5.1 to rewrite the right hand side of the above equation in terms of the ζ-regularized determinant of A,

$$\frac{\partial^2 f_2}{\partial q' \partial b_2} = \left(\frac{m}{2}\det{}_{\zeta} A\right) \cdot \frac{\partial q}{\partial b_2}$$

All that is left to do is to solve for $\partial q/\partial b_2$ and plugging the results back into equation (2.72). Doing so yields the statement in equation 2.71. □

The following corollary is an immediate consequence of the above theorem and the prior work from section 2.6,

Corollary 2.6.1. *The lattice-regularize determinant and ζ-regularized determinant of A relate in the following manner,*

$$\det{}_{reg} A = \frac{1}{2}\det{}_{\zeta} A$$

The above corollary, illustrates that the lattice-regularization is a viable alternative to the ζ-regularization for the determinants of operators that arise in the Gelfand-Yaglom type formulas. For the operator A above, we see that the regularizations are only off by a constant factor. Moreover, the lattice-regularization amounts to a relatively simple exercise in derivatives (so long as the operator is not too complicated).

Chapter 3

Kasteleyn Operators

We now turn our attention to a problem regarding dimer models. Specifically, we spend our time studying the inverse Kasteleyn operator for a partially non-periodic weighting of the infinite square lattice. We begin in section 3.1 by discussing the necessary preliminary information and the definition of the Kasteleyn operator. This is followed by section 3.2, where we will go over some well known solutions in the periodic case that will be important for understanding the motivation for the lattice weights chosen in section 3.3. Section 3.3 is dedicated to defining the Kasteleyn operator with interface and computing an asymptotic form of the inverse operator. Lastly, in section 3.4 we use asymptotic methods to describe the local behavior of the Kasteleyn operator in various regions of the lattice.

3.1 Defining the Kasteleyn operator

In this section, we aim to define the Kasteleyn operator on a simple, bipartite graph (possibly infinite). While the graph need not be bipartite to define the Kasteleyn operator, we will only consider such cases in this exposition.

Let $G = (B, W, E)$ be any planar bipartite graph, where E denotes the set of edges and we partition the vertices into the set of black, B, and white, W, vertices. We first equip our graph with edge weights. For any edge, $e \in E$, we assign a weight $wt(e) \in \mathbb{R}_{>0}$. Suppose the edge e connects the vertex v to the vertex u, then we use the notation $wt(e) = wt(u, v) = wt(v, u)$ to denote the edge weight interchangeably. There is no direction associated to the edge weight.

Next, we assign an orientation to our graph, which we call a Kasteleyn orientation. For the purpose of this exposition, it suffices to exhibit a Kasteleyn orientation on the square lattice. Figure 3.1 gives an example of a Kasteleyn orientation on a portion of the square lattice. Moreover, this will be our choice of orientation throughout this paper. Given a

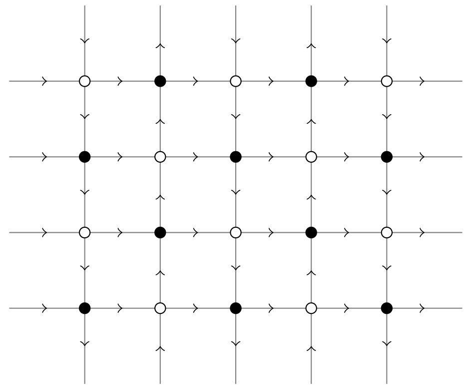

Figure 3.1: Example of a Kasteleyn orientation on the square lattice.

Kasteleyn orientation of a graph G we define the function $s : V \times V \to \mathbb{R}$ by,

$$s(v,u) = \begin{cases} 0 & \text{if there is no edge between } v \text{ and } u \\ 1 & \text{if there is an edge between } v \text{ and } u \text{ orientated from } v \text{ to } u \\ -1 & \text{if there is an edge between } v \text{ and } u \text{ orientated from } u \text{ to } v \end{cases} \tag{3.1}$$

Now we have all the information necessary to define the Kasteleyn operator.

Definition 3.1 (Kasteleyn operator). *given a graph G, the Kasteleyn operator $K(G; wt, s) : V \to V$ is defined by,*

$$K(G; wt, s)v = \sum_{u \sim v} s(v,u)wt(v,u)u \tag{3.2}$$

where the sum is taken over all vertices that neighbor v.

We will sometimes simplify the notation and use $K := K(G; wt, s)$ when the choice of graph, edge weights, and orientation is clear. Two different choices of Kasteleyn orientation will result in Kasteleyn operators that are gauge equivalent.

When G is bipartite, it is useful to think of the Kasteleyn operator as acting on the space $B \oplus W$, where it has the structure

$$K(G; wt, s) = \begin{pmatrix} 0 & -\tilde{K}(G; wt, s)^t \\ \tilde{K}(G; wt, s) & 0 \end{pmatrix} \tag{3.3}$$

where $\tilde{K}(G; wt, s) : B \to W$ is the restriction of the Kasteleyn operator to the black vertices. Notice from this structure that the Kasteleyn operator, K, is skew-symmetric on a bipartite graph. Again we will use the notation, $\tilde{K} := \tilde{K}(G; wt, s)$, when the choice of graph, edge weights, and orientation is clear. By choosing an identification of $B \simeq W$, for example a reference perfect matching, we can consider objects like the determinant of $\tilde{K}$. With this in mind, it suffices to consider just the operator $\tilde{K}$ when studying objects like the determinant and inverse of K.

The Kasteleyn operator is a central object in the study of dimer configurations (analogously tilings) on bipartite graphs. The following theorem is a central result in the literature,

Theorem (Kasteleyn [11], Temperley and Fisher [24])**.** *For a bipartite graph with $wt(e) = 1$ for all $e \in E$ and any Kasteleyn orientation, the number of perfect matchings is equal to $\sqrt{\det K}$ (where we take the positive root). Equivalently, the number of perfect matchings is equal to $|\det \tilde{K}|$.*

For graphs with arbitrary edge weights, the Kasteleyn operator and its inverse also give us information on the probability that a set of edges are simultaneously covered in an arbitrary dimer model. This is detailed in the following theorem,

Corollary (Kenyon [13])**.** *Given a set of edges of a bipartite planar graph, $X = \{e(w_1, b_1), \ldots, e(w_k, b_k)\}$, the probability that all edges in X are covered in a given dimer covering is,*

$$\left(\prod_{i=1}^{k} K(b_i, w_i)\right) \det \left(K^{-1}(w_i, b_j)\right)_{1 \leq i,j \leq k} \tag{3.4}$$

where the coefficient $K(b, w)$ is defined by, $\tilde{K}b = \sum_w K(b, w)w$ (and likewise for the inverse coefficients).

Given a set of two edges, we define their dimer correlation function to be the difference between their joint probability (of being covered) and the product of their individual probabilities (of being covered). If we consider the two edges to be $e(w_1, b_1)$ and $e(w_2, b_2)$ then, by the corollary above, the correlation function is proportional to $K^{-1}(w_1, b_2)K^{-1}(w_2, b_1)$.

In general, as two edges become further away from each other in a model, we expect them to become less correlated. The components of the inverse Kasteleyn operator inform us on how quickly the correlation functions decay.

This leads us to introduce another way of determining the phase in a certain region of the model. It is known that the asymptotic behavior of the *correlation function* between two dimers behaves predictably given the phase of the region of the model. In particular, the correlation functions are deterministic in the deterministic regions, decay inversely with respect to the square distance in the critical regions, and decay exponentially with respect to the distance in the non-critical regions. While the correlation functions are local in nature, they give an alternate method for understanding the phases and limit shape of the dimer model. All of these facts show us that one way to understand the local statistics of a dimer model is to understand the entries of the inverse Kasteleyn operator. This will be aim in sections 3.3 and 3.4 of this exposition.

3.2 Periodic weights and the Kasteleyn operator

We will consider the Kasteleyn operator on the infinite square lattice with periodic weights and periodic boundary conditions. In these instance, it is useful to define the fundamental domain of the lattice. Utilizing the fundamental domain will allow us to understand local dimer statistics of the model without having to go through what are well-known, but often long, computations.

Uniform weights

First we will consider the uniform weights, $wt(e) = 1$ for all $e \in E$. Figure 3.2 depicts the 2×2 fundamental domain of this lattice. The fundamental domain consists of two black vertices vertices, $b_\uparrow(n,m)$ and $b_\downarrow(n,m)$, and two white vertices, $w_\uparrow(n,m)$ and $w_\downarrow(n,m)$. The coordinates (n,m) denote the particular fundamental domain the vertices belong to.

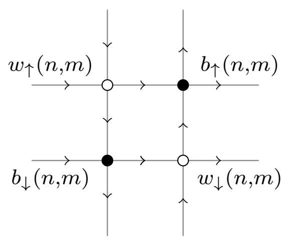

Figure 3.2: The fundamental domain of the lattice with uniform edge weights.

Our goal is to compute the inverse Kasteleyn operator of this fundamental example. It will suffice to just compute the inverse of $\tilde{K}$. We start off by computing how $\tilde{K}$ acts on the two black vertices of an arbitrary fundamental domain,

$$\tilde{K}b_\uparrow(n,m) = w_\uparrow(n+1,m) - w_\uparrow(n,m) + w_\downarrow(n,m+1) - w_\downarrow(n,m) \tag{3.5}$$

$$\tilde{K}b_\downarrow(n,m) = -w_\uparrow(n,m) + w_\uparrow(n,m-1) + w_\downarrow(n,m) - w_\downarrow(n-1,m) \tag{3.6}$$

Since the lattice is translationally invariant in the n and m directions, we can Fourier transform equations (3.5) and (3.6). We will let z and ω denote the Fourier variables in the n and m directions, respectively. We define the Fourier transform of the $b_i(n,m)$ and $w_i(n,m)$ functions as,

$$B_i(z,\omega) = \sum_{n,m} b_i(n,m) z^{-n}\omega^{-m} \tag{3.7}$$

$$W_i(z,\omega) = \sum_{n,m} w_i(n,m) z^{-n}\omega^{-m} \tag{3.8}$$

where $i = \uparrow, \downarrow$. Plugging these into equations (3.5) and (3.6) gives,

$$\tilde{K}_{z,\omega}B_\uparrow(z,\omega) = (z-1)W_\uparrow(z,\omega) + (\omega-1)W_\downarrow(z,\omega) \tag{3.9}$$

$$\tilde{K}_{z,\omega}B_\downarrow(z,\omega) = (\omega^{-1}-1)W_\uparrow(z,\omega) + (1-z^{-1})W_\downarrow(\omega,z) \tag{3.10}$$

Using the above, we can write a matrix form of $\tilde{K}_{z,w}$,

$$\tilde{K}_{z,w} = \begin{pmatrix} z-1 & w^{-1}-1 \\ w-1 & 1-z^{-1} \end{pmatrix} \tag{3.11}$$

Inverting the above matrix directly gives,

$$\left(\tilde{K}_{z,\omega}\right)^{-1} = \frac{1}{z+z^{-1}+w+w^{-1}-4} \begin{pmatrix} 1-z^{-1} & 1-w^{-1} \\ 1-w & z-1 \end{pmatrix} \tag{3.12}$$

where $\left(\tilde{K}_{z,\omega}\right)^{-1} : W \to B$. Using the inverse Fourier transform will yield a double integral form for the coefficients of the inverse Kasteleyn. Since the lattice is translationally invariant, it suffices to fix one of the vertices at the fundamental domain $(0,0)$. Let's take a look at the integral form of $\tilde{K}^{-1}\left(w_\uparrow(0,0), b_\downarrow(n,m)\right)$,

$$\tilde{K}^{-1}\left(w_\uparrow(0,0), b_\downarrow(n,m)\right) = \frac{1}{4\pi^2}\int_{|z|=1}\int_{|w|=1} \frac{(1-w)z^n w^m}{z+z^{-1}+w+w^{-1}-4}\frac{dw}{iw}\frac{dz}{iz} \tag{3.13}$$

Choosing different vertices of the fundamental domain would simply change the numerator of the integrand according to the appropriate entry of equation (3.12).

Next, we consider the asymptotic behavior of $\tilde{K}^{-1}\left(w_\uparrow(0,0), b_\downarrow(n,m)\right)$ as n and m become large. We will first approach this using integral methods. Let $\omega = e^{i\theta}$ and rewrite the denominator in (3.13) as,

$$(z+z^{-1}+w+w^{-1}-4)z = (z-\lambda_-)(z+\lambda_+) \tag{3.14}$$

where,

$$\lambda_\pm = \frac{1}{2}\left(4-2\cos\theta \pm \sqrt{(2\cos\theta-4)^2-4}\right)$$

We then use the residue theorem to handle the integral with respect to z, and we are left with an integral with respect to θ. We use asymptotic techniques on this integral and we find that $\tilde{K}^{-1}\left(w_\uparrow(0,0), b_\downarrow(n,m)\right)$ decays inversely with respect to the distance. We refer to this lattice as *critical* because of this decay rate.

The spectral curve of the dimer model

We can see from the above analysis of $\tilde{K}^{-1}\left(w_\uparrow(0,0), b_\downarrow(n,m)\right)$ that the asymptotic behavior depends on whether the roots, $\lambda_\pm$, lie inside or outside the unit circle. Moreover, these roots appear in the denominator of equation (3.13) which is, in fact, the determinant of $\tilde{K}_{z,w}$ once we choose an identification, $B \simeq W$. We choose the identification which associates $b_\uparrow(n,m) \simeq w_\uparrow(n,m)$ and $b_\downarrow(n,m) \simeq w_\downarrow(n,m)$ for all n and m. With this in mind we compute,

$$\det \tilde{K}_{z,w} = p(z,w) = z+z^{-1}+w+w^{-1}-4 \tag{3.15}$$

We call the function $p(z, w)$ the *spectral curve* of the dimer model because it's roots tell us about the spectrum of the Kasteleyn operator and consequently the behavior of the correlation functions [15]. We refer to the lattice model as being *critical* (rough) if the entries of the inverse Kasteleyn operator decay inversely with respect to distance. We say that the lattice is *non-critical* (smooth) if the entries of the inverse Kasteleyn operator decay exponentially with respect to distance.

For periodic weightings and boundary conditions, we can determine whether the lattice model is critical by simply observing the roots of the spectral curve. If the roots of $p(z, w)$ lie on the unit torus, then the lattice is critical, otherwise the lattice is non-critical. In the next section we will look at a richer example to illustrate this fact more completely.

A periodic weighting

Let's now consider the periodic weighting given by the fundamental domain in figure 3.3. Using the process described in section 3.2, we can write the 2×2 matrix $\tilde{K}_{z,\omega}$,

$$\tilde{K}_{z,\omega} = \begin{pmatrix} z-1 & b\omega^{-1}-a \\ a\omega - b & 1-z^{-1} \end{pmatrix} \tag{3.16}$$

and compute the determinant using the same identification that was discussed in section 3.2,

$$\det \tilde{K}_{z,\omega} = p(z,\omega) = -2 - 2ab + b^2\omega^{-1} + a^2\omega + z^{-1} + z \tag{3.17}$$

The asymptotic behavior of the entries of the inverse Kasteleyn depend on the roots of the above function. Moreover, the roots depend on the value of the positive parameters a and b. If we fix the value of z on the unit torus, $|p(z,\omega)|$ is minimal for $\omega = 1$. Applying this we

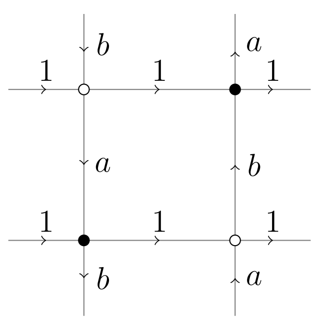

Figure 3.3: A periodic weighting on the 2×2 fundamental domain. We label the domain vertices in the same manner as figure 3.2.

are left with,

$$0 = (a-b)^2 - 2 + z + z^{-1} \tag{3.18}$$

Thus, $p(z,\omega)$ has solutions on the unit torus if and only if $|a-b| < 2$. So the lattice weights are critical when $|a-b| < 2$ and non-critical when $|a-b| > 2$. The fact that the above lattice can be made critical or non-critical by changing the values of a and b is the motivation for the lattice we will describe in the next section.

3.3 Kasteleyn operator with interface

In this section, we will introduce a new weighting on the infinite square lattice that is periodic only in one direction. We will refer to this lattice as the *square lattice with interface* and to the corresponding Kasteleyn operator as the *Kasteleyn operator with interface*. We will compute an integral form for the inverse Kasteleyn operator with interface. Later on, in section 3.4, we will consider the asymptotic behavior of this integral form to determine the local statistics of the lattice.

Square lattice with interface

To understand the square lattice with interface, it will be useful to understand a coordinate system on the lattice. In the horizontal and vertical directions we will enumerate every other face of the lattice, such that each vertex is associated to exactly one enumerated face. The vertical direction will be known as the m-direction, while the horizontal direction will be known as the n-direction. Thus every enumerated face, and the four vertices associated to it, will have the coordinates (n, m). These coordinates on the lattice are depicted in figure 3.4. On the square lattice with interface, each enumerated face with $n \leq 0$ will have edge

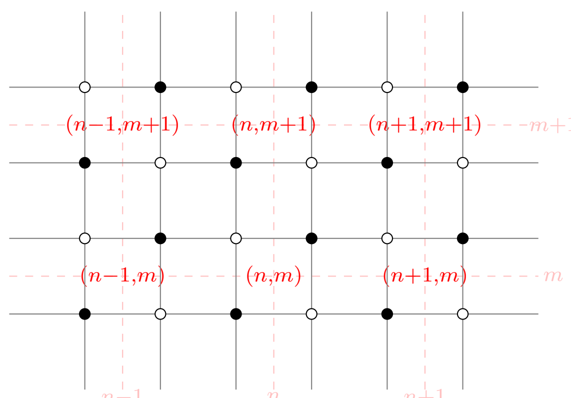

Figure 3.4: Coordinates on the bipartite square lattice. Note that the face and the four adjacent vertices are all denoted by the given coordinate.

weights defined by figure 3.3 and enumerated faces where $n > 0$ will have edge weights defined by figure 3.6. Since the change of weights occurs at $n = 0$, we call this line in the lattice *the interface*. The depiction of the lattice near the interface is shown in figure 3.5. The aim of this 'interface' weighting is to choose an appropriate a and b such that the two halves of the lattice exhibit different fundamental behavior. In particular, we are interested in the case where $b - a > 2$, because one might expect half the lattice to behave critically while the other half behaves non-critically. From this set up, we can explicitly define what we mean by the Kasteleyn operator with interface,

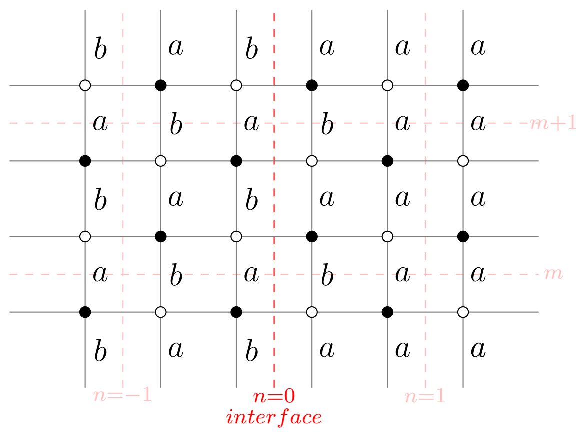

Figure 3.5: The planar, bipartite square lattice with interface at $n = 0$. All unlabeled edges have weight one. We also equipped this lattice with the Kasteleyn orientation depicted in figure 3.1.

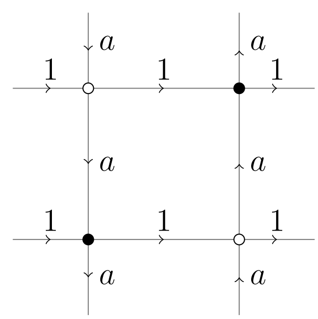

Figure 3.6: The edge weights surrounding ennumerated faces when $n > 0$.

Definition 3.2 (Kasteleyn operator with interface)**.** *Let G be the square lattice with interface defined in figure 3.5 equipped with the Kasteleyn orientation depicted in figure 3.1. We define the Kasteleyn operator with interface to be,*

$$K_{int} := \tilde{K}(G) \tag{3.19}$$

Again, since we are using the operator $\tilde{K}$, it is important to mention that we use the same identification of $B \simeq W$ as was described in section 3.2. Since we aim to compute the inverse of the Kasteleyn operator with interface, we need to comment on the boundary conditions of the lattice. In the m-direction, we will assume periodic boundary conditions since the lattice in translationally invariant in this direction. In the n-directions, instead of applying typical boundary conditions we will apply conditions of convergence directly to the inverse Kasteleyn. These conditions will be seen in action in the proof of Theorem 1.

Inverse Kasteleyn with interface

In this section, we will state an explicit integral form of the entries of the inverse Kasteleyn operator with interface defined above. Before stating we first define the following functions with variable ω,

$$z_1(\omega) = a\omega - b \tag{3.20}$$

$$z_2(\omega) = a(\omega - 1) \tag{3.21}$$

$$r_{i,\pm}(\omega) = \frac{1}{2\omega}\left(2\omega + z_i(\omega)^2 \pm z_i(\omega)\sqrt{z_i(\omega)^2 - 4\omega}\right) \tag{3.22}$$

and the following vector valued function,

$$\mathbf{v}_{i,\pm}(\omega) = \begin{pmatrix} \omega^{-1} z_i(\omega) \\ r_{i,\pm}(\omega) - 1 \end{pmatrix} \tag{3.23}$$

where $r_{i,\pm}(\omega)$ and $\mathbf{v}_{i,\pm}(\omega)$ are defined for $i = 1, 2$. Although the above functions explicitly depend on ω, we will simplify the notation where it does not create confusion. In these instances we will let,

$$z_i := z_i(\omega)$$
$$r_{i,\pm} := r_{i,\pm}(\omega)$$
$$\mathbf{v}_{i,\pm} := \mathbf{v}_{i,\pm}(\omega)$$

With these functions in mind we can now define the functions central to the inverse Kasteleyn operator with interface,

$$\begin{pmatrix} G^{>}_{\uparrow\uparrow}(n, n_o; \omega) \\ G^{>}_{\downarrow\uparrow}(n, n_0; \omega) \end{pmatrix} = \begin{cases} c_1(n_0;\omega)\mathbf{v}_{1,+}(\omega) r_{1,+}(\omega)^n & n \leq 0 \\ c_2(n_0;\omega)\mathbf{v}_{2,+}(\omega) r_{2,+}(\omega)^n + c_3(n_0;\omega)\mathbf{v}_{2,-}(\omega) r_{2,-}(\omega)^n & 0 < n \leq n_0 \\ c_4(n_0;\omega)\mathbf{v}_{2,-}(\omega) r_{2,-}(\omega)^n & n > n_0 \end{cases} \tag{3.24}$$

$$\begin{pmatrix} G^{>}_{\uparrow\downarrow}(n, n_0; \omega) \\ G^{>}_{\downarrow\downarrow}(n, n_0; \omega) \end{pmatrix} = \begin{cases} d_1(n_0;\omega)\mathbf{v}_{1,+}(\omega) r_{1,+}(\omega)^n & n \leq 0 \\ d_2(n_0;\omega)\mathbf{v}_{2,+}(\omega) r_{2,+}(\omega)^n + d_3(n_0;\omega)\mathbf{v}_{2,-}(\omega) r_{2,-}(\omega)^n & 0 < n < n_0 \\ d_4(n_0;\omega)\mathbf{v}_{2,-}(\omega) r_{2,-}(\omega)(\omega)^n & n \geq n_0 \end{cases} \tag{3.25}$$

$$\begin{pmatrix} G^{<}_{\uparrow\uparrow}(n, n_0; \omega) \\ G^{<}_{\downarrow\uparrow}(n, n_0; \omega) \end{pmatrix} = \begin{cases} c'_1(n_0;\omega)\mathbf{v}_{1,+}(\omega) r_{1,+}(\omega)^n & n \leq n_0 \\ c'_2(n_0;\omega)\mathbf{v}_{1,+}(\omega) r_{1,+}(\omega)^n + c'_3(n_0;\omega)\mathbf{v}_{1,-}(\omega) r_{1,-}(\omega)^n & n_0 < n \leq 0 \\ c'_4(n_0;\omega)\mathbf{v}_{2,-}(\omega) r_{2,-}(\omega)^n & n > 0 \end{cases} \tag{3.26}$$

$$\begin{pmatrix} G^{<}_{\uparrow\downarrow}(n, n_0; \omega) \\ G^{<}_{\downarrow\downarrow}(n, n_0; \omega) \end{pmatrix} = \begin{cases} d'_1(n_0;\omega)\mathbf{v}_{1,+}(\omega) r_{1,+}(\omega)^n & n < n_0 \\ d'_2(n_0;\omega)\mathbf{v}_{1,+}(\omega) r_{1,+}(\omega)^n + d'_3(n_0;\omega)\mathbf{v}_{1,-}(\omega) r_{1,-}(\omega)^n & n_0 \leq n \leq 0 \\ d'_4(n_0;\omega)\mathbf{v}_{2,-}(\omega) r_{2,-}(\omega)^n & n > 0 \end{cases} \tag{3.27}$$

where the coefficients $c_i(n_0;\omega)$, $c'_i(n_0;\omega)$, $d_i(n_0;\omega)$, and $d'_i(n_0;\omega)$ are defined in the Appendix B. The vertices $w_\uparrow(n,m)$, $w_\downarrow(n,m)$, $b_\uparrow(n,m)$, and $b_\downarrow(n,m)$ are the same vertices described in figure 3.2.

Theorem 3.1 (Inverse Kasteleyn operator with interface)**.** *The inverse to the Kasteleyn operator with interface has the integral form,*

$$K_{int}^{-1}\left(w_i(n_0,0),b_j(n,m)\right)=\begin{cases}\dfrac{1}{2\pi}\displaystyle\int_{|\omega|=1}G_{ij}^{>}(n,n_0;\omega)\omega^m\frac{d\omega}{i\omega} & n_0>0\\ \dfrac{1}{2\pi}\displaystyle\int_{|\omega|=1}G_{ij}^{<}(n,n_0;\omega)\omega^m\frac{d\omega}{i\omega} & n_0<0\end{cases}\tag{3.28}$$

where $i=\uparrow,\downarrow$, $j=\uparrow,\downarrow$. *Since the lattice is translationally invariant in the* m*-direction we fix* $m_0=0$ *without loss of generality.*

Proof. First let us compute how K_{int} acts on the vertices $b_\uparrow(n,m)$ and $b_\downarrow(n,m)$,

$$K_{\text{int}}b_\uparrow(n,m)=\begin{cases}w_\uparrow(n+1,m)-w_\uparrow(n,m)+aw_\downarrow(n,m+1)-bw_\downarrow(n,m) & n\leq 0\\ w_\uparrow(n+1,m)-w_\uparrow(n,m)+aw_\downarrow(n,m+1)-aw_\downarrow(n,m) & n>0\end{cases}\tag{3.29}$$

$$K_{\text{int}}b_\downarrow(n,m)=\begin{cases}bw_\uparrow(n,m-1)-aw_\uparrow(n,m)+w_\downarrow(n,m)-w_\downarrow(n-1,m) & n\leq 0\\ aw_\uparrow(n,m-1)-aw_\uparrow(n,m)+w_\downarrow(n,m)-w_\downarrow(n-1,m) & n>0\end{cases}\tag{3.30}$$

Since we are applying periodic boundary conditions to the lattice in the m-direction, we can use the Fourier transform on the above. We will let ω to denote the Fourier variable and define,

$$B_\omega^j(n)=\sum_m b_j(n,m)\omega^{-m}$$
$$W_\omega^j(n)=\sum_m w_j(n,m)\omega^{-m}$$

for $j=\uparrow,\downarrow$. We can now rewrite equations (3.29) and (3.30) using the Fourier variable,

$$K_{\text{int}}(n;\omega)B_\omega^\uparrow(n)=\begin{cases}W_\omega^\uparrow(n+1)-W_\omega^\uparrow(n)+z_1(\omega)W_\omega^\downarrow(n) & n\leq 0\\ W_\omega^\uparrow(n+1)-W_\omega^\uparrow(n)+z_2(\omega)W_\omega^\downarrow(n) & n>0\end{cases}\tag{3.31}$$

$$K_{\text{int}}(n;\omega)B_\omega^\downarrow(n)=\begin{cases}-\omega z_1(\omega)W_\omega^\uparrow(n)+W_\omega^\downarrow(n)-W_\omega^\downarrow(n-1) & n\leq 0\\ -\omega z_2(\omega)W_\omega^\uparrow(n)+W_\omega^\downarrow(n)-W_\omega^\downarrow(n-1) & n>0\end{cases}\tag{3.32}$$

The functions $z_1(\omega)$ and $z_2(\omega)$ are defined in equations (3.20) and (3.21). From the above equations we can write $K_{\text{int}}(n;\omega)$ as a (piece-wise) difference operator acting on the vector

$\begin{pmatrix} B_\omega^\uparrow(n) \\ B_\omega^\downarrow(n) \end{pmatrix}$,

$$K_{\text{int}}(n;\omega) = \begin{cases} \begin{pmatrix} D_+ - 1 & -\omega z_1(\omega) \\ z_1(\omega) & 1 - D_- \end{pmatrix} & n \leq 0 \\ \begin{pmatrix} D_+ - 1 & -\omega z_2(\omega) \\ z_2(\omega) & 1 - D_- \end{pmatrix} & n > 0 \end{cases} \tag{3.33}$$

Where $D_\pm$ are the discrete operators defined by, $D_\pm f(n) = f(n \pm 1)$. We are now interested in finding the Green's function of the difference operator above. The Green's function will satisfy,

$$K_{\text{int}}(n;\omega)\mathcal{G}(n,n_0;\omega) = \begin{pmatrix} \delta_{n,n_0} & 0 \\ 0 & \delta_{n,n_0} \end{pmatrix} \tag{3.34}$$

where δ_{n,n_0} is the Kronecker delta. We will use the following notation for the components of $\mathcal{G}(n,n_0;\omega)$,

$$\mathcal{G}(n,n_0;\omega) = \begin{pmatrix} G_{\uparrow\uparrow}(n,n_0;\omega) & G_{\uparrow\downarrow}(n,n_0;\omega) \\ G_{\downarrow\uparrow}(n,n_0;\omega) & G_{\downarrow\downarrow}(n,n_0;\omega) \end{pmatrix} \tag{3.35}$$

In the case where $n \neq n_0$, equation (3.34) can be epressed as two (piece-wise) linear system each pertaining to two components of $\mathcal{G}(n,n_0;\omega)$. These systems can be written as,

$$\begin{pmatrix} G_{\uparrow j}(n+1,n_0;\omega) \\ G_{\downarrow j}(n+1,n_0;\omega) \end{pmatrix} = M_n \begin{pmatrix} G_{\uparrow j}(n,n_0;\omega) \\ G_{\downarrow j}(n,n_0;\omega) \end{pmatrix} \tag{3.36}$$

Where $j = \uparrow, \downarrow$ and

$$M_n = \begin{cases} \begin{pmatrix} 1 & \omega^{-1} z_1(\omega) \\ -z_1(\omega) & 1 - \omega^{-1} z_1(\omega)^2 \end{pmatrix} & n \leq 0 \\ \begin{pmatrix} 1 & \omega^{-1} z_2(\omega) \\ -z_2(\omega) & 1 - \omega^{-1} z_2(\omega)^2 \end{pmatrix} & n > 0 \end{cases} \tag{3.37}$$

We are now able to solve for the Green's function of $K_{\text{int}}(n;\omega)$ by simply stitching together the appropriate linear solutions. For any $|\omega| = 1$ the system above is non-degenerate, so we may solve for the eigenvalues and eigenvalues of the system in terms of ω. The eigenvalues of M_n are given by $r_{1,\pm}(\omega)$ when $n \leq 0$ and $r_{2,\pm}(\omega)$ when $n > 0$. Recall these functions are defined in equation (3.22). The eigenvectors of M_n are given by $\mathbf{v}_{1,\pm}(\omega)$ when $n \leq 0$ and $\mathbf{v}_{2,\pm}(\omega)$ when $n > 0$. Again these vector valued functions are defined in equation (3.23).

Before we write the general solution, we must use our boundary condition in the n-direction. In this direction, we will require that the entries of the inverse Kasteleyn converge as n becomes large in magnitude. It will suffice to define the following constraint on the Green's function as $n \to \pm\infty$,

$$\lim_{n \to \pm\infty} G_{ij}(n,n_0;\omega) = 0 \tag{3.38}$$

For each $i = \uparrow, \downarrow$ and $j = \uparrow, \downarrow$. In order to write a solution that satisfies the above, we should understand the norm of the eigenvalues as ω varies along the unit circle. Figure 3.7 shows plots of the norms of the roots $r_{1,\pm}(\omega)$ given various values of a and b. Note that when $a = b$, $r_{1,\pm}(\omega) = r_{2,\pm}(\omega)$.

With all this in mind, we may write the general solution for the Green's function. Since

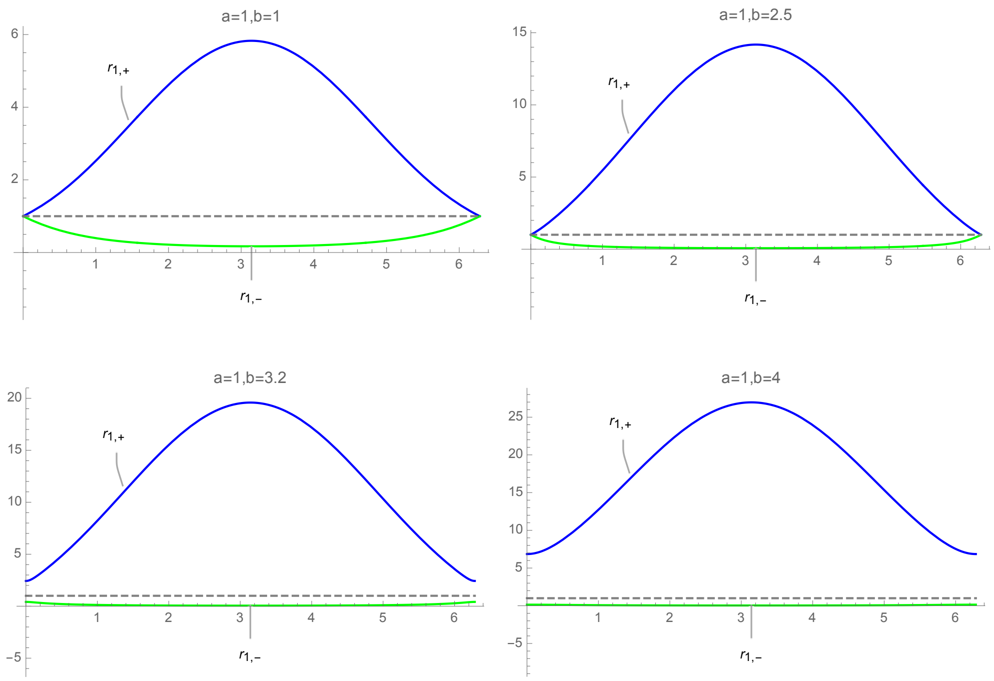

Figure 3.7: The above plots depict the norms of the eigenvalues as ω varies along the unit circle and for various values of a and b. The x-axis indicates the argument of ω. The gray dashed line depicts norm equal to 1. Note that criticality of the weighting can also be seen in these graphs. The system is critical if $|r_{1,+}(\omega)| = |r_{1,-}(\omega)| = 1$ for some $|\omega| = 1$. Thus, the the weighting is critical for the top two plots, and non-critical for the bottom two.

the solution depends on whether $n_0 \leq 0$ or $n_0 > 0$, we will write these solutions are separate cases. We will denote the solutions for when $n_0 \leq 0$ and $n_0 > 0$ by $G^{<}_{ij}(n, n_0; \omega)$ and $G^{>}_{ij}(n, n_0; \omega)$, respectively. The general solutions are repeated below,

$$\begin{pmatrix} G^{>}_{\uparrow\uparrow}(n, n_o; \omega) \\ G^{>}_{\downarrow\uparrow}(n, n_0; \omega) \end{pmatrix} = \begin{cases} c_1(n_0; \omega)\mathbf{v}_{1,+}(\omega) r_{1,+}(\omega)^n & n \leq 0 \\ c_2(n_0; \omega)\mathbf{v}_{2,+}(\omega) r_{2,+}(\omega)^n + c_3(n_0; \omega)\mathbf{v}_{2,-}(\omega) r_{2,-}(\omega)^n & 0 < n \leq n_0 \\ c_4(n_0; \omega)\mathbf{v}_{2,-}(\omega) r_{2,-}(\omega)^n & n > n_0 \end{cases}$$

$$\begin{pmatrix} G^{>}_{\uparrow\downarrow}(n, n_0; \omega) \\ G^{>}_{\downarrow\downarrow}(n, n_0; \omega) \end{pmatrix} = \begin{cases} d_1(n_0; \omega)\mathbf{v}_{1,+}(\omega) r_{1,+}(\omega)^n & n \leq 0 \\ d_2(n_0; \omega)\mathbf{v}_{2,+}(\omega) r_{2,+}(\omega)^n + d_3(n_0; \omega)\mathbf{v}_{2,-}(\omega) r_{2,-}(\omega)^n & 0 < n < n_0 \\ d_4(n_0; \omega)\mathbf{v}_{2,-}(\omega) r_{2,-}(\omega)(\omega)^n & n \geq n_0 \end{cases}$$

$$\begin{pmatrix} G^{<}_{\uparrow\uparrow}(n, n_0; \omega) \\ G^{<}_{\downarrow\uparrow}(n, n_0; \omega) \end{pmatrix} = \begin{cases} c_1'(n_0; \omega)\mathbf{v}_{1,+}(\omega) r_{1,+}(\omega)^n & n \leq n_0 \\ c_2'(n_0; \omega)\mathbf{v}_{1,+}(\omega) r_{1,+}(\omega)^n + c_3'(n_0; \omega)\mathbf{v}_{1,-}(\omega) r_{1,-}(\omega)^n & n_0 < n \leq 0 \\ c_4'(n_0; \omega)\mathbf{v}_{2,-}(\omega) r_{2,-}(\omega)^n & n > 0 \end{cases}$$

$$\begin{pmatrix} G^{<}_{\uparrow\downarrow}(n, n_0; \omega) \\ G^{<}_{\downarrow\downarrow}(n, n_0; \omega) \end{pmatrix} = \begin{cases} d_1'(n_0; \omega)\mathbf{v}_{1,+}(\omega) r_{1,+}(\omega)^n & n < n_0 \\ d_2'(n_0; \omega)\mathbf{v}_{1,+}(\omega) r_{1,+}(\omega)^n + d_3'(n_0; \omega)\mathbf{v}_{1,-}(\omega) r_{1,-}(\omega)^n & n_0 \leq n \leq 0 \\ d_4'(n_0; \omega)\mathbf{v}_{2,-}(\omega) r_{2,-}(\omega)^n & n > 0 \end{cases}$$

All that is left is to solve for the coefficients. To do this, we consider equation (3.34) when $n = 0$, $n = n_0$, and $n = n_0 - 1$. All of the coefficients are explicit stated in Appendix B.

Lastly, to get an explicit formula for the entries of K_{int}^{-1} we simply use the inverse Fourier transform on the above.

$$K_{\text{int}}^{-1}(w_i(n_0, 0), b_j(n, m)) = \frac{1}{2\pi} \int_{|w|=1} G^k_{ij}(n, n_0; \omega)\omega^m \frac{d\omega}{i\omega} \tag{3.39}$$

for any $i =\uparrow, \downarrow$, $j =\uparrow, \downarrow$ and $k =>, <$. Note that k depends on the value of n_0. We are allowed to fix the vertex w_i at $m_0 = 0$ since the lattice is translationally invariant in the m-direction. □

3.4 Asymptotic behavior of the inverse Kasteleyn with interface

In this section, we will compute the asymptotic behavior of $K_{\text{int}}^{-1}(w_i(n, m), b_j(n_0, 0))$ with the goal of understanding the limit shape behavior of the lattice. By determining the decay of the inverse Kasteleyn entries, we will learn whether certain regions of the lattice are critical or non-critical. In the critical case, we expect the decay of the inverse Kasteleyn to be inversely related to the distance, while in the non-critical regions we expect the decay to be exponential in distance.

Throughout this analysis we will assume that the $m_0 = 0$ as the lattice is translationally invariant in the m-direction. We will also assume that $b - a > 2$ as we expect this scenario of weights to produce a lattice with both critical and non-critical regions, which it does.

Asymptotic behavior for large m and fixed n and n_0

First we will consider the asymptotic behavior when n and n_0 are close to the boundary and the vertical distance grows. Regardless of what half of the plane the two vertices are in, the inverse Kasteleyn component decays inversely in m. However, it is worth noting that when one of the vertices lies to the left of the interface, it will contribute a term that decays exponentially in the relevant coordinate, even though these values are fixed. We will elaborate on this more after the statement and proof of the corollary,

Corollary 3.1.1. *For n and n_0 fixed, the inverse Kasteleyn entries have the following asymptotic expansion,*

$$K_{int}^{-1}\left(w_i(n_0,0), b_j(n,m)\right) = \frac{1}{\pi m}\Im\left(\lim_{\theta\to 0^+} G_{ij}^k(n,n_0;e^{i\theta})\right) + \mathcal{O}(m^{-2}) \tag{3.40}$$

as $m \to \infty$. Where $i =\uparrow,\downarrow$, $j =\uparrow,\downarrow$, and $k =>,<$ depending on the value of n_0.

Proof. To start, let's substitute $\omega = e^{i\theta}$ into equation (3.39),

$$K_{\text{int}}^{-1}\left(w_i(n_0,0), b_j(n,m)\right) = \frac{1}{2\pi}\int_0^{2\pi} G_{ij}^k(n,n_0;e^{i\theta})e^{i\theta m}d\theta \tag{3.41}$$

We wish to employ the method of steepest decent to compute the asymptotics of the above. The coefficient $G_{ij}^k(n,n_0;e^{i\theta})$ is well-behaved on the interval $(0,2\pi)$. We only need to be aware of the jump discontinuity at the endpoints.

To start we need to deform the contour in the manner depicted by figure 3.8. Consider the three integrals that arise from breaking the contour into the two vertical components and the one horizontal component. Along the horizontal component, we note that

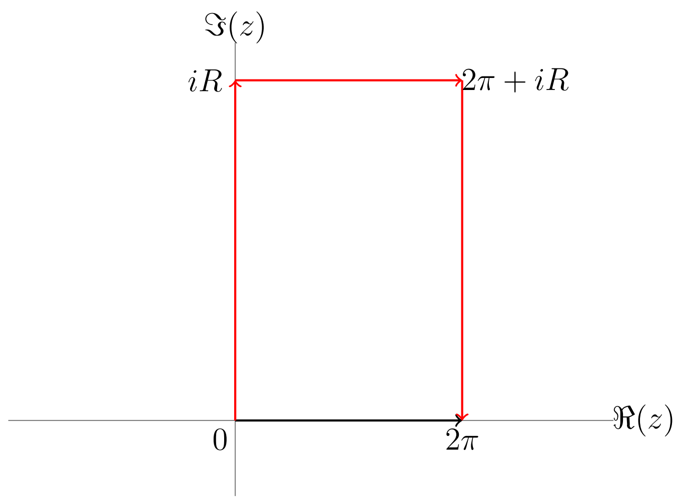

Figure 3.8: For the method of steepest descent we deform the original contour (in black) to the contour in red. Note that we let $R \to \infty$.

$$\left\|G_{ij}^k(n,n_0;e^{-R}e^{is})e^{-Rm}e^{ism}\right\| \leq e^{-R} \tag{3.42}$$

so the integrand vanishes as $R \to \infty$. Now we are left to deal with the integrals along the vertical components of the contour. We write the integral along the left most path as,

$$\lim_{\theta\to 0^+}\frac{i}{2\pi}\int_0^\infty G_{\uparrow\uparrow}^>(n,n_0;e^{-s+i\theta})e^{-sm}ds \tag{3.43}$$

and along the right most path as,

$$-\lim_{\theta\to 2\pi^-}\frac{i}{2\pi}\int_0^\infty G^>_{\uparrow\uparrow}(n,n_0;e^{-s+i\theta})e^{-sm}ds \tag{3.44}$$

Note that we need to take limits due to the discontinuity at the endpoints. Since the exponent is real and decaying, we can now use Laplace's method on both these integrals. Immediately we obtain,

$$K^{-1}_{\text{int}}\left(w_i(n_0,0),b_j(n,m)\right)=\frac{1}{2\pi im}\left(\lim_{\theta_1\to 0^+}G^k_{ij}(n,n_0;e^{i\theta_1})-\lim_{\theta_2\to 2\pi^-}G^k_{ij}(n,n_0;e^{i\theta_2})\right)+\mathcal{O}(m^{-2}) \tag{3.45}$$

Lastly, we can notice that

$$\lim_{\theta_1\to 0^+}G^k_{ij}(n,n_0;e^{i\theta_1})-\lim_{\theta_2\to 2\pi^-}G^k_{ij}(n,n_0;e^{i\theta_2})=2\Im\left(\lim_{\theta\to 0^+}G^k_{ij}(n,n_0;e^{i\theta})\right) \tag{3.46}$$

and so equation (3.45) simplifies to what is given in equation (3.40). □

We would like to take a closer look at the result in Corollary 1 and so it will be useful to consider three specific cases: (1) the case where the vertices both lie to the left of the interface ($n<n_0<0$), (2) the case where the vertices both lie to the right of the interface ($0<n_0<n$), and (3) the case where the vertices lie on opposite sides of the interface ($n_0<0<n$). These cases, and their asymptotics are depicted in figure 3.9. There are certainly more cases we can consider, but looking at these three will be sufficient to understand the behavior around the interface.

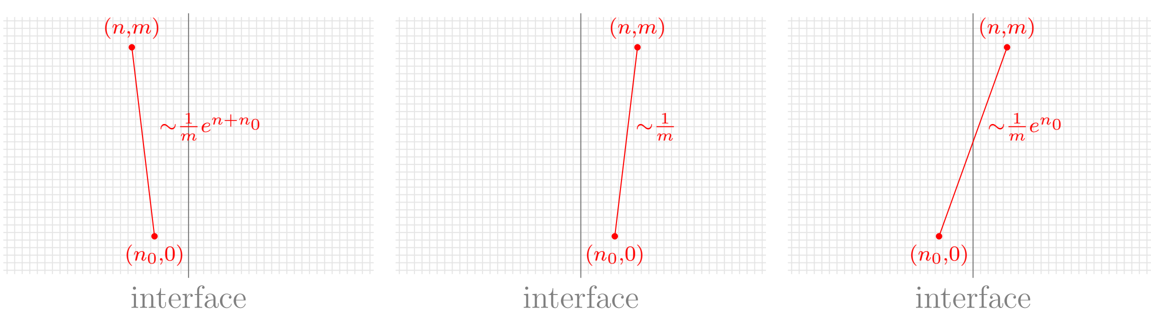

Figure 3.9: The three cases we consider when m is large and n and n_0 are finite. From left to right the cases are, $n<n_0<0$, $0<n_0<n$, and $n_0<0<n$.

In the first case, where $n<n_0<0$, let's compute the leading order term of the expansion of the $\uparrow\uparrow$ case for $a=1$ and $b=4$,

$$K^{-1}_{\text{int}}\left(w_\uparrow(n_0,0),b_\uparrow(n,m)\right)\sim\frac{1}{3m\pi}\left(\frac{-7-3\sqrt{5}}{2}\right)^n\left(\frac{-7+3\sqrt{5}}{2}\right)^{1-n_0} \tag{3.47}$$

And we can see that n and n_0 contribute terms that exponentially decay. The analysis follows suit for the other components (↑↓, ↓↑, and ↓↓) and different values of a and b (so long as $|b-a|>2$).

For the case where $0<n_0<n$ we can also compute the first order term of the expansion for the ↑↑ case where $a=1$ and $b=4$. We find,

$$K_{\text{int}}^{-1}\left(w_{\uparrow}(n_0,0),b_{\uparrow}(n,m)\right)\sim\frac{1}{3m\pi} \tag{3.48}$$

Since both vertices now lie on the right side of the interface, there are no longer exponentially decaying terms and all decay is inverse in m.

And lastly, for the case where $n_0<0<n$ we write out the first order term of the expansion for the ↑↑ case where $a=1$ and $b=4$ as,

$$K_{\text{int}}^{-1}\left(w_{\uparrow}(n_0,0),b_{\uparrow}(n,m)\right)\sim\frac{1}{3m\pi}\left(\frac{-7+3\sqrt{5}}{2}\right)^{-n_0} \tag{3.49}$$

We see that the leading order term decays exponentially in n_0 but not n, since only n_0 lies to the left of the interface. It's important to note that although $n_0<0$, the term being exponentiated has norm less than 1 for any value of a and b such that $|b-a|>2$.

Asymptotic behavior for large horizontal distances

Now we would like to comment on the asymptotic behavior of the inverse Kasteleyn matrix when m is fixed and n and n_0 are manipulated in a way so that the vertices are far away. There are many ways in which we can accomplish this. In this section, we will consider a few methods to compute the asymptotic behavior for large horizontal distances.

Overall, we find that the asymptotic behavior in the horizontal direction depends on which side of the interface the two vertices lie. For example, if both vertices lie on to the left of the interface, the decay will be exponential in the horizontal distance. However, if both vertices lie to the right of the interface, the decay will be linear in the horizontal distance.

Across the interface, n_0 fixed.

First let us consider the case where n_0 is fixed, $|n|\to\infty$, and the two vertices are on opposite sides of the interface. This encompasses two cases where one vertex remains close to the interface while the other vertex is far away. These scenarios are shown in figure 3.10. We expect the asymptotic behavior to be dominated by which side of the interface the vertex indexed by n lies on.

Before stating the results, it will be useful to define what I will call little-g functions. These functions are the result of stripping away the n dependence of $G_{ij}^{k}(n,n;\omega)$ and are only defined for the first and last cases in equations (3.24)-(3.27). For example, when $n_0<0$ and $n>0$ we define,

$$g_{ij,n>0}^{<}(n_0;\omega)r_{2,-}(\omega)^n=G_{ij}^{<}(n,n_0;\omega) \tag{3.50}$$

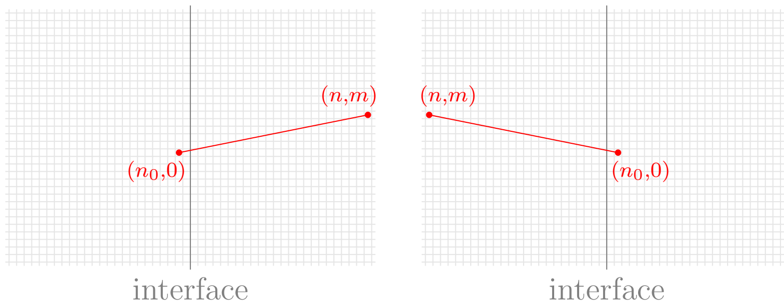

Figure 3.10: The two cases we consider where the vertices are located across the interface and $|n|$ is large.

and for $n < n_0 < 0$ we have,

$$g^{<}_{ij,n<n_0}(n_0;\omega)r_{1,+}(\omega)^n = G^{<}_{ij}(n,n_0;\omega) \tag{3.51}$$

We define the rest of the relevant cases analogously. We will now state two corollaries addressing the scenarios in figure 3.10. First we have,

Corollary 3.1.2. *For $n_0 < 0 < n$ and n_0 and m fixed the inverse Kasteleyn entries have the following asymptotic expansion,*

$$K^{-1}_{int}\left(w_i(n_0,0),b_j(n,m)\right) = \frac{1}{2\pi a n}\left(\lim_{\theta_1\to 0^+} g^{<}_{ij,n>0}(n_0;e^{i\theta_1}) + \lim_{\theta_2\to 2\pi^-} g^{<}_{ij,n>0}(n_0;e^{i\theta_2})\right) + \mathcal{O}(n^{-2}) \tag{3.52}$$

as $n\to\infty$.

Proof. Not that for any $|\omega|=1$, the root $r_{2,-}(\omega)$ is real. Thus solving for the asymptotics of this integral is a direct application of Laplace's method. Plotting the value's of the root over the unit circle (shown in figure 3.11) shows that there are two maximums of equal value ($r_{2,-}(\omega)=1$) at $\theta=0$ and $\theta=2\pi$, where we let $\omega=e^{i\theta}$. We must account for the contributions from both when applying Laplace's method. □

The second case consider is when $n < 0 < n_0$ and thus the vertex indexed by n lies to the left of the interface and in the non-critical region. In this instance we have,

Corollary 3.1.3. *For $n < 0 < n_0$ and n_0 and m fixed the inverse Kasteleyn operator has the following asymptotic expansion,*

$$K^{-1}_{int}\left(w_i(n_0,0),b_j(n,m)\right) = -\frac{1}{\pi}\Im\left(\lim_{\theta\to 0^+} g^{>}_{i,j,n<0}\left(n_0,e^{i\theta}\right)\right)\frac{\sqrt{(a-b)^2-4}}{(a+b)n}e^{nr_{1,+}(1)} + \mathcal{O}\left(\frac{e^{nr_{1,+}(1)}}{n^2}\right) \tag{3.53}$$

as $\to -\infty$.

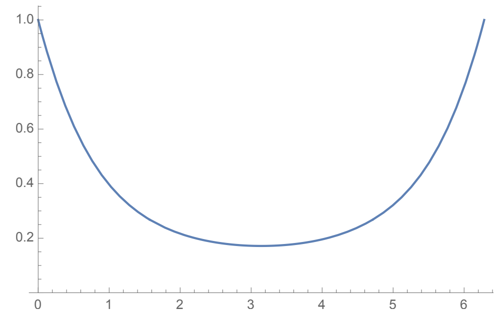

Figure 3.11: Plot of $r_{2,-}(\omega)$ over the unit circle for $a = 1$.

In this case, the asymptotic variable n lies to the left of the interface and thus we get exponential decay that depends on n in the leading order term.

Proof. We cannot immediately apply Laplace's method because the root $r_{1,+}(e^{i\theta})$ is complex. However, if we deform the contour in the manner shown in figure 3.8 we will be able to apply Laplace's method appropriately. With this in mind, the proof now follows the methods used in section 3.4. First we make sure to write,

$$r_{1,+}^n = e^{n \log r_{1,+}} \tag{3.54}$$

where we suppressed the ω dependance in the notation, and we use the series expansion,

$$\log r_{1,+}(e^{-s}) = \log r_{1,+}(1) + \frac{(a+b)}{\sqrt{(a-b)^2 - 4}} s + \mathcal{O}(s^2) \tag{3.55}$$

From this we get the formula stated above in Corollary 3.1.3. □

Critical side of the lattice, n_0 fixed.

Now let's again consider a set up where n_0 is fixed, however now we both vertices will lie to the right of the interface. In particular, $n > n_0 > 0$. The set up is show in figure 3.12. As we see in the corollary below, the asymptotic expansion decays inversely with respect to n in the leading order.

Corollary 3.1.4. *For $n > n_0 > 0$ and m and n_0 are finite, the asymptotic behavior of the inverse Kasteleyn is given by,*

$$K_{int}^{-1}(w_i(n_0, 0), b_j(n, m)) = \frac{1}{\pi a n} \left(\lim_{\theta \to 0^+} g^{>}_{ij,n>n_0}(n_0; e^{i\theta}) \right) + \mathcal{O}(n^{-2}) \tag{3.56}$$

for $i = \uparrow, \downarrow$ and $j = \uparrow, \downarrow$.

Proof. Just like in the case of equation (3.52), this is a direct application of Laplace's method. □

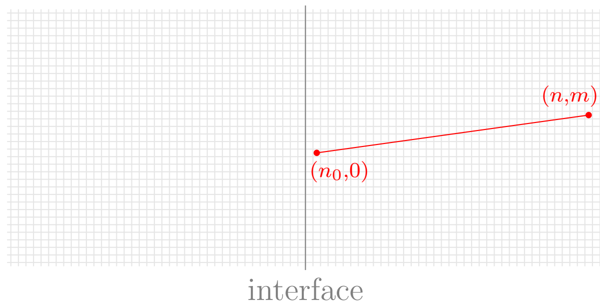

Figure 3.12: The case where both vertices are to the right of the interface, n_0 is finite and n is large.

Non-critical side of the lattice, n_0 fixed

We will consider the complement of the case presented above, that is we will consider the case where $n < n_0 < 0$ and n_0 is fixed and $-n$ becomes large. This scenario is depicted in figure 3.13.

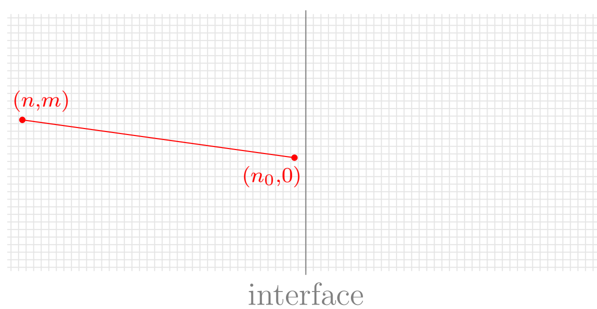

Figure 3.13: The case where both vertices are to the left of the interface, n_0 is fixed, and $-n$ is large.

Corollary 3.1.5. *For $n > n_0 > 0$ and m and n_0 are finite, the asymptotic behavior of the inverse Kasteleyn is given by,*

$$K_{int}^{-1}\left(w_i(n_0,0), b_j(n,m)\right) = -\frac{1}{\pi}\Im\left(\lim_{\theta\to 0^+} g^{<}_{i,j,n<n_0}\left(n_0, e^{i\theta}\right)\right)\frac{\sqrt{(a-b)^2-4}}{(a+b)n}e^{nr_{1,+}(1)} + \mathcal{O}\left(\frac{e^{nr_{1,+}(1)}}{n^2}\right) \tag{3.57}$$

for $i =\uparrow,\downarrow$ and $j =\uparrow,\downarrow$.

Proof. The proof of this corollary follows the same procedure as the proof of equation (3.53). □

Same side of the interface, n and n_0 proportional

Now let's look at the two cases where the vertices are far apart (horizontally) and well to one side of the interface, i.e. neither vertex is fixed by the boundary. The two scenarios of interest are depicted in figure 3.14. To describe the asymptotic behavior succinctly, it will be

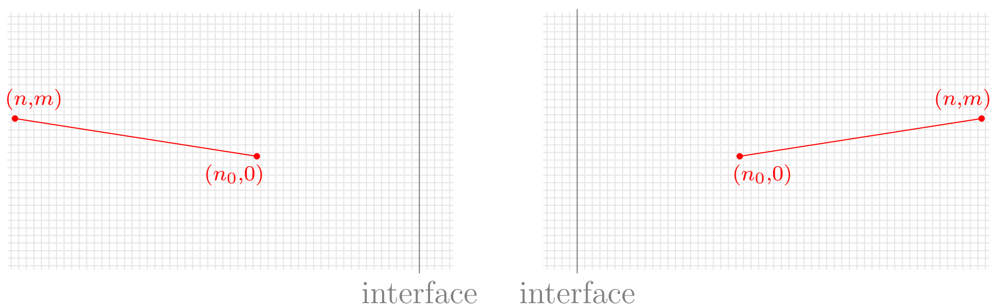

Figure 3.14: The above diagrams depict the cases where n and n_0 lie on the same side of the interface and both indices become large at a proportional rate.

useful to define some notation. We define the coefficients $c_{4,1}(\omega)$, $c_{4,2}(\omega)$, $c'_{1,1}(\omega)$ and $c'_{1,2}(\omega)$ by the equations

$$c_1(\omega) = r_{2,-}(\omega)^{-n_0} c_{4,1}(\omega) + r_{2,+}(\omega)^{-n_0} c_{4,2}(\omega) \tag{3.58}$$

$$c'_1(\omega) = r_{1,+}(\omega)^{-n_0} c'_{1,1}(\omega) + r_{1,-}(\omega)^{-n_0} c'_{1,2}(\omega) \tag{3.59}$$

One should note that the newly defined coefficients have no dependence on n_0. We will first state the corollary describing the asymptotic behavior for when both vertices lie to the right of the interface, in other words the scenario depicted on the right side of figure 3.14.

Corollary 3.1.6. *For $n_0 = N$, $n = pN$ for some $p > 1$, and m finite, the inverse Kasteleyn operator has the following behavior as $N \to \infty$,*

$$K_{int}^{-1}\left(w_\uparrow(n_0,0), b_\uparrow(n,m)\right) = \frac{1}{aN\pi}\left(\frac{1}{p-1}\lim_{\theta\to 0^+} c_{4,1}(e^{i\theta}) z_2(e^{i\theta}) + \frac{1}{p+1}\lim_{\theta\to 0^+} c_{4,2}(e^{i\theta}) z_2(e^{i\theta})\right) + \mathcal{O}(n^{-2}) \tag{3.60}$$

Proof. We need to first split the integral up into two,

$$K_{\text{int}}^{-1}\left(w_i(n_0,0), b_j(n,m)\right) = \frac{1}{2\pi}\int_0^{2\pi} c_{4,1}(e^{i\theta}) z_2(e^{i\theta}) e^{-i\theta} r_{2,-}(e^{i\theta})^{-n_0} r_{2,-}(e^{i\theta})^{n} e^{i\theta m} d\theta + \frac{1}{2\pi}\int_0^{2\pi} c_{4,2}(e^{i\theta}) z_2(e^{i\theta}) e^{-i\theta} r_{2,+}(e^{i\theta})^{-n_0} r_{2,-}(e^{i\theta})^{n} e^{i\theta m} d\theta \tag{3.61}$$

and rewrite them in the following manner,

$$\int_0^{2\pi} c_{4,1}(e^{i\theta})z_2(e^{i\theta})e^{-i\theta}r_{2,-}(e^{i\theta})^{-n_0}r_{2,-}(e^{i\theta})^n e^{i\theta m}d\theta =$$

$$= \int_0^{2\pi} c_{4,1}(e^{i\theta})z_2 e^{i(m-1)\theta}\exp\left(N(p-1)\log r_{2,-}\right)d\theta$$

$$\int_0^{2\pi} c_{4,2}(e^{i\theta})z_2(e^{i\theta})e^{-i\theta}r_{2,+}(e^{i\theta})^{-n_0}r_{2,-}(e^{i\theta})^n e^{i\theta m}d\theta =$$

$$= \int_0^{2\pi} c_{4,2}(e^{i\theta})z_2 e^{i(m-1)\theta}\exp(-N\log r_{2,+} + pN\log r_{2,-})d\theta$$

In both the the above integrals, the function in the exponent has constant imaginary part and the real part decays appropriately. Thus we may use Laplace's method on the two integrals and the result is given by the asymptotic expansion in equation (3.60). □

As expected, 3.1.6 shows us the the inverse Kasteleyn entries decay inversely in N. Now for the case seen in the left most diagram of figure 3.14 we state the following corollary,

Corollary 3.1.7. *For $n_0 = -N$, $n = -pN$ for some $p > 1$, and m finite, the inverse Kasteleyn operator has the following behavior as $N \to \infty$,*

$$K_{int}^{-1}\left(w_\uparrow(n_0,0), b_\uparrow(n,m)\right) =$$

$$= -\frac{\sqrt{(a-b)^2-4}}{\pi(a+b)(1+p)N}\exp(-pN\log r_{1,+}(1) + N\log r_{1,-}(1))\left(\lim_{\theta\to 0^+} c'_{1,2}(e^{i\theta})z_1(e^{i\theta})\right)$$

$$+ \mathcal{O}\left(\frac{\exp(-pN\log r_{1,+}(1) + N\log r_{1,-}(1))}{N^2}\right) \tag{3.62}$$

Proof. Similarly to the work shown in corollary 6, we can expand the one integral into two integrals,

$$\frac{1}{2\pi}\int_0^{2\pi} G^<_{\uparrow\uparrow}(n,n_0;e^{i\theta})e^{im\theta}d\theta =$$

$$= \frac{1}{2\pi}\int_0^{2\pi} c'_{1,1}(e^{i\theta})z_1(e^{i\theta})e^{i(m-1)\theta}\exp(-N(p-1)\log r_{1,+}(e^{i\theta}))d\theta$$

$$+ \frac{1}{2\pi}\int_0^{2\pi} c'_{1,2}(e^{i\theta})z_1(e^{i\theta})e^{i(m-1)\theta}\exp(-pN\log r_{1,+}(e^{i\theta}) + N\log r_{1,-}(e^{i\theta}))d\theta$$

However these exponents are complex, and so we have to deform the contour in the plane. The contour given in figure 3.8 will again work. When we deform the first integral on the right side above, the integrals sum to zero. Thus,

$$\frac{1}{2\pi}\int_0^{2\pi} G^<_{\uparrow\uparrow}(n,n_0;e^{i\theta})e^{im\theta}d\theta =$$

$$= \frac{1}{2\pi}\int_0^{2\pi} c'_{1,2}(e^{i\theta})z_1(e^{i\theta})e^{i(m-1)\theta}\exp(-pN\log r_{1,+}(e^{i\theta}) + N\log r_{1,-}(e^{i\theta}))d\theta$$

Computing the asymptotic expansion of this follows the work detail in 3.1.3. □

Chapter 4

Dirac Operator

In this chapter, we will consider a continuous (two-dimensional) operator that is reminiscent of the Kasteleyn operator with interface described in Chapter 3. This Dirac-like operator is motivated by the result in [14], which proves that the Kasteleyn operator on the uniformly weighted lattice converges to the massless Dirac operator in the continuum limit.

We will start by defining the Dirac operator with interface. We will then compute the Green's function of the operator and look at it's asymptotic behavior in the interesting case where the two points are located across the interface. Lastly, we will draw connections between the results here and those in Chapter 3, as well as draw connections between the operators in question.

4.1 The Dirac operator with interface

Let us start by defining the two-dimensional Dirac operator with interface.

Definition 4.1. *The Dirac operator with interface acts on two component wave functions, $\Psi(x, y) \in L^2(\mathbb{R}^2, \mathbb{C}) \oplus L^2(\mathbb{R}^2, \mathbb{C})$, and is defined by,*

$$\mathcal{D}(x) = \begin{cases} \begin{pmatrix} m_1 & -i\partial_x - \partial_y \\ -i\partial_x + \partial_y & -m_1 \end{pmatrix} & x < 0 \\ \\ \begin{pmatrix} m_2 & -i\partial_x - \partial_y \\ -i\partial_x + \partial_y & -m_2 \end{pmatrix} & x > 0 \end{cases} \tag{4.1}$$

Where m_1, $m_2 \geq 0$.

This definition is immediately inspired by the Kasteleyn operator with interface defined in chapter 3. It was shown in [14] that the Kasteleyn operator on the uniformly weighted lattice converges to the massless Dirac operator.

The goal of this chapter is to compute the Green's function of the above operator and commute the asymptotic behavior of the Green's function as the source and point become far away.

4.2 Green's function of the Dirac operator with interface

Our first goal is to compute an integral form of the Green's function associated with the Dirac operator with interface. This integral form of the Green's function should be reminiscent of the formula for the inverse Kasteleyn computed back in Theorem 3.1.

Let us first be reminded that the Green's function will satisfy the equation,

$$\mathcal{D}(x)\mathcal{G}(x,y;x_0,y_0) = \begin{pmatrix} \delta(x,x_0)\delta(y,y_0) & 0 \\ 0 & \delta(x,x_0)\delta(y,y_0) \end{pmatrix} \tag{4.2}$$

Where $\delta(s,t)$ denotes the Dirac delta distribution centered at $s = t$. Since the operator defined in equation (4.1) is invariant in the y-direction, we should first Fourier transform equation (4.2) in this direction. Doing this we obtain,

$$\mathcal{D}(x|q)\mathcal{G}(x,x_0|q) = \begin{pmatrix} \delta(x,x_0) & 0 \\ 0 & \delta(x,x_0) \end{pmatrix} \tag{4.3}$$

where,

$$\mathcal{D}(x|q) = \begin{cases} \begin{pmatrix} m_1 & -i\partial_x - iq \\ -i\partial_x + iq & -m_1 \end{pmatrix} & x < 0 \\ \begin{pmatrix} m_2 & -i\partial_x - iq \\ -i\partial_x + iq & -m_2 \end{pmatrix} & x > 0 \end{cases} \tag{4.4}$$

and we denote the components of the transformed Green's function by,

$$\mathcal{G}(x,x_0|q) = \begin{pmatrix} G_{11}(x,x_0|q) & G_{12}(x,x_0|q) \\ G_{21}(x,x_0|q) & G_{22}(x,x_0|q) \end{pmatrix} \tag{4.5}$$

We define the following function of q,

$$\epsilon_i(q) = \sqrt{q^2 + m_i^2} \tag{4.6}$$

for $i = 1, 2$. We can now express the form of the transformed Green's function, $\mathcal{G}(x, x_0|q)$ when we fix $x_0 > 0$.

$$\mathcal{G}(x,x_0|q) = \begin{cases} \begin{pmatrix} ic_1(q)\big(q+\epsilon_1(q)\big) & id_1(q)\big(q+\epsilon_1(q)\big) \\ c_1(q)m_1 & d_1(q)m_1 \end{pmatrix} e^{\epsilon_1(q)x} & x<0 \\ \begin{pmatrix} ic_2(q)\big(q+\epsilon_2(q)\big) & id_2(q)\big(q+\epsilon_2(q)\big) \\ c_2(q)m_2 & d_2(q)m_2 \end{pmatrix} e^{\epsilon_2(q)x} & \\ \quad + \begin{pmatrix} ic_3(q)\big(q-\epsilon_2(q)\big) & id_3(q)\big(q-\epsilon_2(q)\big) \\ c_3(q)m_2 & d_3(q)m_2 \end{pmatrix} e^{-\epsilon_2(q)x} & 0<x<x_0 \\ \begin{pmatrix} ic_4(q)\big(q-\epsilon_2(q)\big) & id_4(q)\big(q-\epsilon_2(q)\big) \\ c_4(q)m_2 & d_4(q)m_2 \end{pmatrix} e^{-\epsilon_2(q)x} & x>x_0 \end{cases} \tag{4.7}$$

Note the the coefficients $c_i(q)$ and $d_i(q)$ for $i = 1, 2$ seen above are defined in appendix C. We now state the theorem which defines the integral form of the Green's function for the Dirac operator with interface,

Theorem 4.1 (Green's function for the Dirac operator with interface)**.** *When we fix some* $x_0 > 0$*, the Green's function for the Dirac operator with interface has the integral form,*

$$\mathcal{G}(x, y; x_0, 0) = \frac{1}{2\pi}\int_{-\infty}^{\infty} \mathcal{G}(x, x_0|q)e^{iqy}dq \tag{4.8}$$

where we define the integration above to be component-wise.

Note that in the above theorem we are allowed to set $y_0 = 0$ without loss of generality because the operator is translationally invariant in the y-direction. Moreover, the case when we fix $x_0 < 0$ follows the work done here with minor adjustments. We will not compute this case in this exposition for brevity.

Proof. To solve the system in (4.3), we should first note that the solution depends on whether $x_0 < 0$ or $x_0 > 0$. In this proof, we will only focus on the case where $x_0 > 0$. For the former case, the proof follows a similar set up so we will omit it. For $x_0 > 0$, we will consider the solution in the domains $x < 0$, $0 < x < x_0$, and $x > x_0$ and stitch the solutions together using the appropriate conditions. Note we also need to consider the boundary conditions on the lattice as $|x| \to \infty$. In particular, we will assume that $G_{jk}(x, x_0|q) \to 0$ as $|x| \to 0$ for $j = 1, 2$ and $k = 1, 2$.

Let's first consider the solution to (4.3) in the domain where $x < 0$. In this domain, equation (4.3) can be expressed as,

$$\begin{pmatrix} m_1 & -i\partial_x - iq \\ -i\partial_x + iq & -m_1 \end{pmatrix} \begin{pmatrix} G_{11}(x, x_0|q) & G_{12}(x, x_0|q) \\ G_{21}(x, x_0|q) & G_{22}(x, x_0|q) \end{pmatrix} = \begin{pmatrix} 0 & 0 \\ 0 & 0 \end{pmatrix} \tag{4.9}$$

The general solution to the above is,

$$\mathcal{G}(x,x_0|q) = \begin{pmatrix} ic_1(q+\epsilon_1(q)) & id_1(q+\epsilon_1(q)) \\ c_1 m_1 & d_1 m_1 \end{pmatrix} e^{\epsilon_1(q)x} + \begin{pmatrix} ic_2(q-\epsilon_1(q)) & id_2(q-\epsilon_1(q)) \\ c_2 m_1 & d_2 m_1 \end{pmatrix} e^{-\epsilon_1(q)x} \tag{4.10}$$

We need to consider the general solution under the conditions stated for $x \to -\infty$. Taking these into account, we can eliminate the second matrix term above.

$$\mathcal{G}(x,x_0|q) = \begin{pmatrix} ic_1(q+\epsilon_1(q)) & id_1(q+\epsilon_1(q)) \\ c_1 m_1 & d_1 m_1 \end{pmatrix} e^{\epsilon_1(q)x} \tag{4.11}$$

We can apply the same procedure for finding the solution in the domains $0 < x < x_0$ and $x > x_0$. The general solution when $0 < x < x_0$ is

$$\mathcal{G}(x,x_0|q) = \begin{pmatrix} ic_2(q+\epsilon_2(q)) & id_2(q+\epsilon_2(q)) \\ c_2 m_2 & d_2 m_2 \end{pmatrix} e^{\epsilon_2(q)x} + \begin{pmatrix} ic_3(q-\epsilon_1(q)) & id_3(q-\epsilon_1(q)) \\ c_3 m_2 & d_3 m_2 \end{pmatrix} e^{-\epsilon_2(q)x} \tag{4.12}$$

Note we reused the coefficients c_2 and d_2 above since they did not end up appearing in (4.11). The solution for when $x > x_0$, which takes into account the appropriate boundary conditions, is

$$\mathcal{G}(x,x_0|q) = \begin{pmatrix} ic_4(q-\epsilon_2(q)) & id_4(q-\epsilon_2(q)) \\ c_4 m_2 & d_4 m_2 \end{pmatrix} e^{-\epsilon_2(q)x} \tag{4.13}$$

We now want to stitch together the general solutions described by equations (4.11)-(4.13) to solve for the unknown coefficients. Note that in actuality, the coefficients are functions of q with parameter x_0, so from here on we will use the notation $c_i(q)$ and $d_i(q)$, where $i = 1, 2, 3, 4$.

To solve for the coefficients we should first make sure that equation (4.11) and (4.12) agree when $x = 0$, as the Green's function should be continuous across the interface. We then need to stitch together the solution appropriately when $x = x_0$. Because of the delta distributions the components $G_{11}(x, x_0|q)$ and $G_{22}(x, x_0|q)$ should be continuous at $x = x_0$, however this will not be the case for $G_{12}(x, x_0|q)$ and $G_{21}(x, x_0|q)$. The details for solving for the coefficients, and their explicit form can be found in Appendix C.

All that's left to do is use the inverse Fourier transform to get an expression for the original Green's function. Doing this results in the integral given in the statement of Theorem 4.1. □

The massive-massless interface

We are particularly interested in the case where $m_1 > 0$ and $m_2 = 0$. In other words, the interface separates a massive Dirac operator and a massless Dirac operator. In this instance, we can easily give an explicit integral form of the Green's function. To do so let's first define the notation we will use for the Heaviside function,

$$H(x) = \begin{cases} 1 & x > 0 \\ 0 & x < 0 \end{cases} \tag{4.14}$$

We define the following function, which we denote $\mathcal{G}_{m_1,0}(x, x_0|q)$.

$$\mathcal{G}_{m_1,0}(x,x_0|q) = \begin{cases} \begin{pmatrix} \frac{-(\epsilon_1(q)+q)}{m_1}H(-q) & -iH(q) \\ iH(-q) & \frac{-m_1}{\epsilon_1(q)+q}H(q) \end{pmatrix} e^{\epsilon_1(q)x-|q|x_0} & x < 0 \\ -i\begin{pmatrix} 0 & H(q) \\ H(-q) & 0 \end{pmatrix} e^{|q|(x-x_0)} \\ \qquad + \begin{pmatrix} \frac{\epsilon_1(q)+q}{m_1}H(-q) & 0 \\ 0 & \frac{-m_1}{\epsilon_1(q)+q}H(q) \end{pmatrix} e^{-|q|(x+x_0)} & 0 < x < x_0 \\ i\begin{pmatrix} 0 & H(-q) \\ H(q) & 0 \end{pmatrix} e^{-|q|(x-x_0)} \\ \qquad + \begin{pmatrix} \frac{-(\epsilon_1(q)+q)}{m_1}H(-q) & 0 \\ 0 & \frac{-m_1}{\epsilon_1(q)+q} \end{pmatrix} e^{-|q|(x+x_0)} & x > x_0 \end{cases} \tag{4.15}$$

This leads us to the following corollary,

Corollary 4.1.1. *The Green's function for the Dirac operator with a massive-massless interface has the integral form,*

$$\mathcal{G}_{m_1,0}(x, y; x_0, 0) = \frac{1}{2\pi}\int_{-\infty}^{\infty} \mathcal{G}_{m_1,0}(x, x_0|q)e^{iyq}dq \tag{4.16}$$

Proof. The function $\mathcal{G}_{m_1,0}(x, x_0|q)$ is derived by taking the limit of $\mathcal{G}(x, x_0|q)$ as $m_2 \to 0$. The result immediately follows. □

4.3 Asymptotics of the Green's function

We would like to compute the asymptotics of the Green's function, $\mathcal{G}_{m_1,0}(x, y; x_0, 0)$, for the case when the two points lie on opposite sides of the interface. In particular, it will suffice to study the case where $x < 0$ and $x_0 > 0$. This case is depicted in figure 4.1. The asymptotics are neatly described in the following corollary,

Corollary 4.1.2. *Let $x = -(ay + c)$ and $x_0 = by + d$, where a, b, c, and d are non-negative (real) constants. The Green's function for the Dirac operator with massive-massless interface*

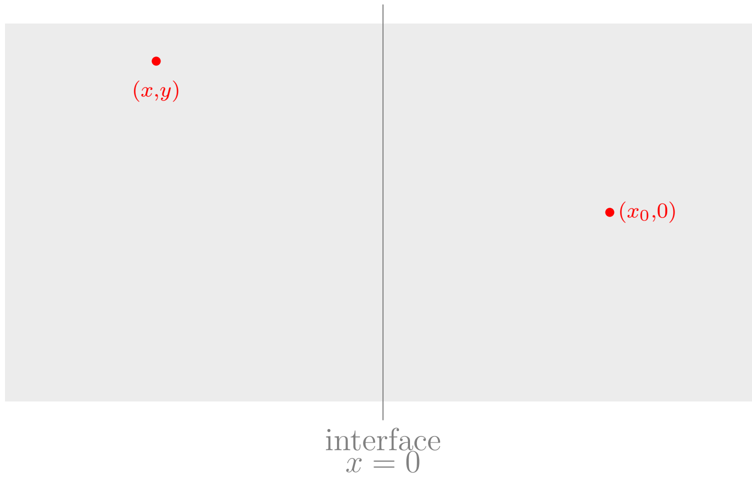

Figure 4.1: The case where the two points lie on opposite sides of the interface.

has the following leading order behavior

$$\mathcal{G}_{m_1,0}(x,y;x_0,0) = \begin{pmatrix} \frac{1}{b+i} & \frac{i}{b-i} \\ \frac{-i}{b+i} & \frac{-1}{b-i} \end{pmatrix} \frac{e^{xm_1}}{2\pi y} + \begin{pmatrix} \frac{-1-dm_1}{m_1(b+i)^2} & \frac{id}{(b-i)^2} \\ \frac{id}{(b+i)^2} & \frac{1+dm_1}{m_1(b-i)^2} \end{pmatrix} \frac{e^{xm_1}}{2\pi y^2} + O\left(e^{xm_1}y^{-3}\right) \tag{4.17}$$

as y tends to positive infinity.

Proof. To compute the asymptotic behavior, we will consider the proof for two cases. First we will consider the special case where $a = b = 0$. In this case, both vertices are close to the interface and the vertical distance between them is large. After that, we will consider the more general case where either $a \neq 0$, $b \neq 0$, or both.

The asymptotics should be computed component-wise, although the procedure for each component is the same. In this proof, we will prove the asymptotics for the $(1,1)$-component of the matrix. We will refer to this component as $G_1 1(x,y;x_0,0)$ and the Fourier transformed version as $G_1 1(x,x_0|q)$. Even though we are dropping the $m_1, 0$ subscript for conciseness, we will be working strictly with the Green's function for the Dirac operator with massive-massless interface.

Let's start by simplifying the expression in equation (4.16) and restricting to the case of G_{11}. This yields the integral,

$$G_{11}(x,y;x_0,0) = \frac{1}{2\pi m_1} \int_{-\infty}^{0} (q + \epsilon_1(q))\, e^{\epsilon_1(q)x + qx_0} e^{iqy} dq \tag{4.18}$$

Notice that the first exponential does not depend on the asymptotic parameter, y. We would like to use Watson's lemma to approximate the above integral, however we must first deform the contour so that the exponential part that depends on y has a decaying real part. We will deform the contour so it sits along the positive imaginary axis. Doing so, we obtain

$$G_{11}(x, y; x_0, 0) = \frac{1}{2\pi i m_1} \int_0^\infty \left(is + \sqrt{m_1^2 - s^2} \right) e^{\sqrt{m_1^2 - s^2}x + isx_0} e^{-sy} ds \tag{4.19}$$

Now we will approximate the part of the integrand that is not dependent on y by using its Taylor series about $s = 0$.

$$\left(is + \sqrt{m_1^2 - s^2} \right) e^{\sqrt{m_1^2 - s^2}x + isx_0} = m_1 e^{m_1 x} + i(1 + m_1 x_0) e^{m_1 x} s + O(s^2) \tag{4.20}$$

Using the above approximation and Watson's lemma we obtain,

$$G_{11}(x, y; x_0, 0) = \frac{-i}{2\pi y} e^{m_1 x} + \frac{1 + m_1 x_0}{2\pi m_1 y^2} e^{m_1 x} + O\left(y^{-3} \right) \tag{4.21}$$

Which agrees with equation (4.17). The leading order of the decay of the above function is inversely related to the asymptotic variable y. While there is an exponential term that depends on x, since x is fixed in this instance the term is effectively a constant.

We now need to consider the case where either a or b is non-zero (or both). In this case, the integral form of G_{11} looks like,

$$G_{11}(x, y; x_0, 0) = \int_{-\infty}^{0} f(q) e^{g(q)y} dq \tag{4.22}$$

where,

$$f(q) = \frac{1}{2\pi m_1} \left(q + \epsilon_1(q) \right) e^{-\epsilon_1(q)c + qd} \tag{4.23}$$

$$g(q) = -a\epsilon_1(q) + bq + iq \tag{4.24}$$

Note that, on the domain $(-\infty, 0]$, both functions are maximum at $q = 0$. Moreover, the function $e^{g(q)y}$ decays exponentially as $q \to -\infty$. We can series expand both $f(q)$ and $g(q)$,

$$f(q) = \frac{1}{2\pi} e^{-cm_1} + \frac{1 + dm_1}{2\pi m_1} e^{-cm_1} q + Q(q^2) \tag{4.25}$$

$$g(q) = -am_1 + (b + i)q + O(q^2) \tag{4.26}$$

And using the first few terms of these expansion, we can approximate the integral with Laplace's method,

$$G_{11}(x, y; x_0, 0) = \frac{1}{b + i} \frac{e^{xm_1}}{2\pi y} - \frac{1 + dm_1}{m_1(b + i)^2} \frac{e^{xm_1}}{2\pi y^2} + O\left(e^{m_1 x} y^{-3} \right) \tag{4.27}$$

Again the above agrees with the Corollary. Note that now the decay is exponential, because x depends linearly on y. The proof for the other components of the Green's function follow the same procedure and thus we omit them. □

4.4 Connections to the Kasteleyn operator

We can immediately draw similarities between the asymptotic behavior of the Dirac operator with massive-massless interface to the asymptotic behavior of the Kasteleyn operator with (non-critical/critical) interface. In particular, we can compare Corollaries 4.1.2, 3.1.2, and 3.1.1 to see that the asymptotic behavior is the same for the two operators in these instances.

Because of these similarities, it is reasonable to ask if the Kasteleyn operator with (non-critical/critical) interface converges in the continuum limit to the Dirac operator with massive-massless interface. This is not true, and we can see this through a simple computation.

We will simply consider the Kasteleyn operator that results from the lattice weighting where the fundamental domain is given by figure 3.3. It will be useful to employ the notation,

$$f(n,m) = \begin{pmatrix} b_\uparrow(n,m) \\ b_\downarrow(n,m) \\ w_\uparrow(n,m) \\ w_\downarrow(n,m) \end{pmatrix} \tag{4.28}$$

The Kasteleyn operator has the form,

$$Kf(n,m) = \begin{pmatrix} w_\uparrow(n+1,m) - w_\uparrow(n,m) + a\left(w_\downarrow(n,m+1) - w_\downarrow(n,m)\right) \\ -b\left(w_\uparrow(n,m) - w_\uparrow(n,m-1)\right) + w_\downarrow(n,m) - w_\downarrow(n-1,m) \\ b_\uparrow(n+1,m) - b_\uparrow(n,m) - b\left(b_\downarrow(n,m+1) - b_\downarrow(n,m)\right) \\ a\left(b_\uparrow(n,m) - b_\uparrow(n,m-1)\right) + b_\downarrow(n+1,m) - b_\downarrow(n,m) \end{pmatrix} + \begin{pmatrix} (a-b)w_\downarrow(n,m) \\ (b-a)w_\uparrow(n,m) \\ (a-b)b_\downarrow(n,m) \\ (b-a)b_\uparrow(n,m) \end{pmatrix} \tag{4.29}$$

The above is expressed in a manner that will make it easier to compute the continuum limit. We will equipped the lattice, $\mathbb{Z}^2$, with a mesh size of ϵ and let $x = \epsilon n$ and $y = \epsilon m$. In the continuum limit the Kasteleyn operator becomes,

$$Kf(x,y) = \begin{pmatrix} 0 & 0 & \partial_x & a\partial_y \\ 0 & 0 & -b\partial_y & \partial_x \\ \partial_x & -b\partial_y & 0 & 0 \\ a\partial_y & \partial_x & 0 & 0 \end{pmatrix} f(x,y) + \epsilon^{-1} \begin{pmatrix} 0 & 0 & 0 & a-b \\ 0 & 0 & b-a & 0 \\ 0 & a-b & 0 & 0 \\ b-a & 0 & 0 & 0 \end{pmatrix} f(x,y) \tag{4.30}$$

In the case where $a = b$ we get,

$$Kf = \begin{pmatrix} 0 & 0 & \partial_x & a\partial_y \\ 0 & 0 & -a\partial_y & \partial_x \\ \partial_x & -a\partial_y & 0 & 0 \\ a\partial_y & \partial_x & 0 & 0 \end{pmatrix} \tag{4.31}$$

and

$$K^2 = \begin{pmatrix} \partial_x^2 + a^2\partial_y^2 & 0 & 0 & 0 \\ 0 & \partial_x^2 + a^2\partial_y^2 & 0 & 0 \\ 0 & 0 & \partial_x^2 + a^2\partial_y^2 & 0 \\ 0 & 0 & 0 & \partial_x^2 + a^2\partial_y^2 \end{pmatrix} \tag{4.32}$$

So up to appropriate scaling this is essentially a massless Dirac operator. However, when $a \neq b$ we do not immediately recover the massive Dirac operator. Moreover, we see that there is a singular part which appears in (4.30).

While the work in chapters 3 and 4 shows a deep connection between the Kasteleyn operator with interface and the Dirac operator with interface, more work needs to be done to show the relationship between these two operators. In particular, it would be beneficial to find a Kasteleyn type operator on the lattice which immediately converges to the massive Dirac operator. It would then be worthwhile to study the connection between this Kasteleyn-like operator and the Kasteleyn operator used here.

Appendix A

Proof of Lemma 2.1.1

In this appendix we will prove Lemma 2.1.1 which is essential in the proof of theorem 2.1. For this proof, we will assume the matrices $\partial^2 H/\partial \vec{p}_i^{\,2}$ are invertible for all $i = 1, \ldots, n$. Under this assumption, we can use the Schur complement to help us express the determinant of $\tilde{A}_N$,

$$\det(\tilde{A}_N) = \det(D_1)\det(D_4 - D_3 D_1^{-1} D_2)$$

where the matrices D_i for $i = 1, 2, 3, 4.$ are described by equation (2.24). The matrix $D_4 - D_3 D_1^{-1} D_2$ is a block tridiagonal matrix and so we can use techniques described in [20] to compute the determinant of the matrix. We compute,

$$\det(D_4 - D_3 D_1^{-1} D_2) = (-1)^{Nm} \det(T_{11}^{(0)}) \det(B_1 \cdots B_{N-1})$$

The matrices B_i for $i = 1, \ldots, N-1$ are defined in equation (2.40) and the matrix $T_{11}^{(0)}$ is given by,

$$T_{11}^{(0)} = V_2^T T_{N-1} \cdots T_2 V_1$$

where T_i for $i = 2, \ldots, N-1$ are defined by equation (2.36). Lemma 1 follows immediately from the above.

Appendix B

Computation of the coefficients in Theorem 3.1

Below we explicitly state the coefficients present in the Green's function of the Kasteleyn operator with interface that is given in equations (3.24)-(3.27). While most of the functions presented here are dependent on the parameter ω, we drop the notation to fit the equations nicely on the page.

$$c_1 = \frac{(1 - r_{2,-})r_{2,+}^{-n_0}\omega}{r_{1,+}z_1(-1 + r_{2,-}) + r_{2,-}z_2(1 - r_{1,+})} \tag{B.1}$$

$$c_2 = \frac{(-1 + r_{2,-})r_{2,+}^{-n_0}\omega}{z_2(r_{2,+} - r_{2,-})} \tag{B.2}$$

$$c_3 = \frac{(-1 + r_{2,-})r_{2,+}^{-n_0}\omega\,(r_{1,+}z_1(1 - r_{2,+}) + r_{2,+}z_2(-1 + r_{1,+}))}{(r_{2,-} - r_{2,+})z_2\,(r_{1,+}z_1(1 - r_{2,-}) + r_{2,-}z_2(-1 + r_{1,+}))} \tag{B.3}$$

$$c_4 = \frac{r_{2,-}^{-n0}(-1 + r_{2,+})\omega}{z_2(r_{2,+} - r_{2,-})} + c_3 \tag{B.4}$$

$$d_1 = -\frac{r_{2,-}r_{2,+}^{1-n_0}z_2}{r_{1,+}z_1(1 - r_{2,-}) + r_{2,-}z_2(-1 + r_{1,+})} \tag{B.5}$$

$$d_2 = \frac{r_{2,-}r_{2,+}^{1-n_0}}{r_{2,-} - r_{2,+}} \tag{B.6}$$

$$d_3 = \frac{r_{2,-}r_{2,+}^{1-n_0}\,(r_{1,+}z_1(-1 + r_{2,+}) + r_{2,+}z_2(1 - r_{1,+}))}{(r_{2,+} - r_{2,-})\,(r_{1,+}z_1(-1 + r_{2,-}) + r_{2,-}z_2(1 - r_{1,+}))} \tag{B.7}$$

$$d_4 = \frac{r_{2,+}r_{2,-}^{-n_0+1}}{r_{2,-} - r_{2,+}} + d_3 \tag{B.8}$$

$$c'_1 = \frac{(-1 + r_{1,-})r_{1,+}^{-n_0}\omega}{(r_{1,+} - r_{1,-})z_1} + c'_2 \tag{B.9}$$

$$c'_2 = \frac{r_{1,-}^{-n_0}(-1 + r_{1,+})\omega\,(r_{1,-}z_1(-1 + r_{2,-}) + r_{2,-}z_2(1 - r_{1,-}))}{(r_{1,-} - r_{1,+})z_1\,(r_{1,+}z_1(-1 + r_{2,-}) + r_{2,-}z_2(1 - r_{1,+}))} \tag{B.10}$$

$$c'_3 = \frac{r_{1,-}^{-n_0}(-1 + r_{1,+})\omega}{(r_{1,+} - r_{1,-})z_1} \tag{B.11}$$

$$c'_4 = \frac{r_{1,-}^{-n_0}(-1 + r_{1,+})\omega}{r_{1,+}z_1(1 - r_{2,-}) + r_{2,-}z_2(-1 + r_{1,+})} \tag{B.12}$$

$$d'_1 = \frac{r_{1,-}r_{1,+}^{1-n0}}{r_{1,-} - r_{1,+}} + d'_2 \tag{B.13}$$

$$d'_2 = \frac{r_{1,-}^{1-n_0}r_{1,+}\,(r_{1,-}z_1(-1 + r_{2,-}) + r_{2,-}z_2(1 - r_{1,-})))}{(r_{1,+} - r_{1,-})\,(r_{1,+}z_1(-1 + r_{2,-}) + r_{2,-}z_2(1 - r_{1,+}))} \tag{B.14}$$

$$d'_3 = \frac{r_{1,-}^{1-n_0}r_{1,+}}{r_{1,-} - r_{1,+}} \tag{B.15}$$

$$d'_4 = \frac{r_{1,-}^{1-n_0}r_{1,+}z_1}{r_{1,+}z_1(-1 + r_{2,-}) + r_{2,-}z_2(1 - r_{1,+})} \tag{B.16}$$

Appendix C

Computation of coefficients in Theorem 4.1

Here we will explicitly compute the coefficients $c_i(q)$ and $d_i(q)$ for the transformed Green's function given by equation (4.7). First we get four equations from the continuity of the component of $\mathcal{G}(x, x_0|q)$ at $x = 0$. These equations are,

$$ic_1(q)\big(q + \epsilon_1(q)\big) = ic_2(q)\big(q + \epsilon_2(q)\big) + ic_3(q)\big(q - \epsilon_2(q)\big) \tag{C.1}$$

$$c_1(q)m_1 = c_2(q)m_2 + c_3(q)m_2 \tag{C.2}$$

$$id_1(q)\big(q + \epsilon_1(q)\big) = id_2(q)\big(q + \epsilon_2(q)\big) + id_3(q)\big(q - \epsilon_2(q)\big) \tag{C.3}$$

$$d_1(q)m_1 = d_2(q)m_2 + d_3(q)m_2 \tag{C.4}$$

Next we get two equations for the continuity of $G_{11}(x, x_0|q)$ and $G_{22}(x, x_0|q)$ at $x = x_0$,

$$ic_2(q)\big(q + \epsilon_2(q)\big)e^{\epsilon_2(q)x_0} + ic_3(q)\big(q - \epsilon_2(q)\big)e^{-\epsilon_2(q)x_0} = ic_4(q)\big(q - \epsilon_2(q)\big)e^{-\epsilon_2(q)x_0} \tag{C.5}$$

$$d_2(q)m_2e^{\epsilon_2(q)x_0} + d_3(q)m_2e^{-\epsilon_2(q)x_0} = d_4(q)m_2e^{-\epsilon_2(q)x_0} \tag{C.6}$$

Lastly, we have two equations that express the discontinuity of $G_{12}(x, x_0|q)$ and $G_{21}(x, x_0|q)$ at $x = x_0$,

$$id_4(q)\big(q - \epsilon_2(q)\big)e^{-\epsilon_2(q)x_0} - id_2(q)\big(q + \epsilon_2(q)\big)e^{\epsilon_2(q)x_0} - id_3(q)\big(q - \epsilon_2(q)\big)e^{-\epsilon_2(q)x_0} = i \tag{C.7}$$

$$c_4(q)m_2e^{-\epsilon_2(q)x_0} - c_2(q)m_2e^{\epsilon_2(q)x_0} - c_3(q)m_2e^{-\epsilon_2(q)x_0} = i \tag{C.8}$$

The eight equations given by (C.1)-(C.8) are a linear system for the coefficients $c_i(q)$ and $d_i(q)$ for $i = 1, 2, 3, 4$. Solving this system yields,

$$c_1(q) = \frac{i(\epsilon_2(q) - q)}{m_1(\epsilon_2(q) - q) + m_2(\epsilon_1(q) + q)} e^{-\epsilon_2(q)x_0} \tag{C.9}$$

$$c_2(q) = \frac{-i(\epsilon_2(q) - q)}{2\epsilon_2(q)m_2} e^{-\epsilon_2(q)x_0} \tag{C.10}$$

$$c_3(q) = \frac{-i(\epsilon_2(q) - q)\big(m_1(\epsilon_2(q) + q) - m_2(\epsilon_1(q) + q)\big)}{2\epsilon_2(q)m_2\big(m_1(\epsilon_2(q) - q) + m_2(\epsilon_1(q) + q)\big)} e^{-\epsilon_2(q)x_0} \tag{C.11}$$

$$c_4(q) = \frac{i(\epsilon_2(q) + q)}{2\epsilon_2(q)m_2} e^{\epsilon_2(q)x_0} - \frac{i(\epsilon_2(q) - q)\big(m_1(\epsilon_2(q) + q) - m_2(\epsilon_1(q) + q)\big)}{2\epsilon_2(q)m_2\big(m_1(\epsilon_2(q) - q) + m_2(\epsilon_1(q) + q)\big)} e^{-\epsilon_2(q)x_0} \tag{C.12}$$

$$d_1(q) = \frac{-m_2}{m_1(\epsilon_2(q) - q) + m_2(\epsilon_1(q) + q)} e^{-\epsilon_2(q)x_0} \tag{C.13}$$

$$d_2(q) = \frac{-1}{2\epsilon_2(q)} e^{-\epsilon_2(q)x_0} \tag{C.14}$$

$$d_3(q) = \frac{-m_1(\epsilon_2(q) + q) + m_2(\epsilon_1(q) + q)}{2\epsilon_2(q)\big(m_1(\epsilon_2(q) - q) + m_2(\epsilon_1(q) + q)\big)} e^{-\epsilon_2(q)x_0} \tag{C.15}$$

$$d_4(q) = \frac{-1}{2\epsilon_2(q)} e^{\epsilon_2(q)x_0} + \frac{-m_1(\epsilon_2(q) + q) + m_2(\epsilon_1(q) + q)}{2\epsilon_2(q)\big(m_1(\epsilon_2(q) - q) + m_2(\epsilon_1(q) + q)\big)} e^{-\epsilon_2(q)x_0} \tag{C.16}$$

Bibliography

[1] A Borodin. "Schur process and cylindrical partitions". In: *Duke Math. J* 140 (2007), pp. 391–468.

[2] C Boutillier et al. "Dimers on Rail Yard Graphs". In: *Ann. Inst. Henri Poincaré Comb. Phys. Interact* 4 (2017), pp. 479–539.

[3] A Bufetov and V Gorin. "Fluctuations of particle systems determined by Schur generating functions". In: *Adv. Math* 338 (2018), pp. 702–781.

[4] D Burghelea, L Friedlander, and L Kappeler. "On the Determinant of Elliptic Boundary Value Problems on a Line Segement". In: *Proceedings of the American Mathematical Society* 123 (1995).

[5] S Chhita and K Johansson. "Domino statistics of the two-periodic Aztec diamond". In: *Advances in Mathematics* 294 (2016), pp. 37–149.

[6] S Chhita, K Johansson, and B Young. "Asymptotic domino statistics in the Aztec diamond". In: *Ann. Appl. Probab* 25 (3 2015), pp. 1232–1278.

[7] H Cohn, N Elkies, and J Propp. "Local statistics for random domino tilings of the Aztec diamond". In: *Duke Math. J* 85 (1996), pp. 117–166.

[8] C Fulton and S Pruess. "Eigenvalue and Eigenfunction Asymptotics for Regular Sturm-Liouville Problems". In: *Journal of Mathematical Analysis and Applications* 188 (1991).

[9] IM Gelfand and AM Yaglom. "Integration in functional spaces and it applications in quantum physics". In: *Journal of Mathematical Physics* 1 (1960). DOI: 10.1063/1.1703636.

[10] K Johansson. "The Arctic circle boundary and the Airy process". In: *The Ann. of Prob* 33 (2005).

[11] P Kasteleyn. "Graph theory and crystal physics". In: *Graph Theory and Theoretical Physics*. Academic Press, London, 1967, pp. 43–110.

[12] R Kenyon. "Dominoes and the Gaussian free field". In: *Ann. of Prob* 29 (2001), pp. 1128–1137.

[13] R Kenyon. "Local statistics of lattice dimer". In: *Ann. Inst. H. Poincaré Prob* 33 (1997), pp. 591–618.

[14] R Kenyon. "The Laplacian and Dirac operators on critical planar graphs". In: *Inventiones mathematicae* 150 (2002), pp. 409–439.

[15] R Kenyon, A Okounkov, and S Sheffield. "Dimers and Amoebae". In: *Ann. Math* 163 (2006), pp. 1019–1056.

[16] R Kenyon, A Okounkov, and S Sheffield. "Limit shapes and the complex Burgers equation". In: *Acta Mathematica* 199 (2007), pp. 263–302.

[17] K Kirsten. "Functional determinants in higher dimensions using contour integrals". In: *A Window into Zeta and Modular Physics*. Vol. 57. MSRI Publications, 2010, pp. 307–328.

[18] BM Levitan and IS Sargsyan. *Sturm-Liouville and Dirac Operators*. Kluwer Academic Publishers, 1991.

[19] Z Li. "Conformal invariance of dimer heights on isoradial double graphs". In: *Ann. Inst. Henri Poincaré Comb. Phys. Interact* 4 (2017), pp. 273–307.

[20] LG Molinari. "Determinants of block tridiagonal matrices". In: *Linear Algebra and its Applications* 429 (2008), pp. 2221–2226.

[21] A Okounkov and N Reshetikhin. "Correlation function of Schur process with application to local geometry of a random 3-dimensional Young diagram". In: *J. Amer. Math. Soc* 16 (2003), pp. 581–603.

[22] S Sheffield. "Gaussian free field for mathematicians". In: *Prob. Theory Relat. Fields* 139 (2007), pp. 521–541.

[23] LA Takhtajan. *Quantum Mechanics for Mathematicians*. American Mathematical Society, 2008.

[24] HNV Temperley and M Fisher. "Dimer problem in statistical mechanics–an exact result". In: *Philosophical Magazine* 6.8 (1961), pp. 1061–1063.